Ultrasonics 116 (2021) 106471

Contents lists available at ScienceDirect

Ultrasonics

journal homepage: www.elsevier.com/locate/ultras

A review of recent advances in the single- and multi-degree-of-freedom ultrasonic piezoelectric motors

Roland Ryndzionek *, Łukasz Sienkiewicz

Gdansk University of Technology, Faculty Of Electrical And Control Engineering, Gdansk, Poland

ARTICLE INFO

Keywords:
Piezoelectric motor
Traveling wave motor
Ultrasonic
Multi-DOF
Direct drive

ABSTRACT

In this paper a comprehensive review of recent studies on the ultrasonic piezoelectric motors is presented. The authors focus on research articles published in the last five years mostly. The primary subject of this investigation is the development of piezoelectric ultrasonic motors including analytical, numerical and experimental analysis. In further sections, classification methods of piezoelectric motors, survey criteria and three main groups of ultrasonic piezoelectric motors with examples have been presented and described. Finally, the conclusions and future research perspectives have been proposed.

1. Introduction

Since the introduction of the first commercial ultrasonic transducer, a growing interest in the advancement of piezoelectric actuators and motors has been observed. Various new piezoelectric structures have been developed since then[1–5]. Thus, researchers recognize a real renaissance of this technology [6–11]. In general, the penetration of piezoelectric technology reaches almost all fields of engineering technology today e.g. automotive, aerospace, precision manufacturing, optical scanning, bio-technology and medicine [12–18] as well as energy harvesting [19–22].

Developments in the ultrasonic actuator and motor technology are possible thanks to on-going research in the active materials development, especially considering novel high power and low loss ceramics and polymers [23–29]. Active materials that exhibit a significant and useful piezoelectric effect fall into three main groups: natural and synthetic crystals, polarized piezoelectric ceramics, and certain polymer films.

The most widely used piezoelectric material is ferroelectric ceramic - a polycrystalline ceramics like barium titanate (BaTiO3) and lead zirconate titanate (PZT) being the most common examples [30–33]. Among the existing piezoelectric materials, hard PZT ceramics have the highest ability for application in the field of actuators, motors, or motion stages [34–37]. Moreover, the increase of theoretical power density thanks to advances in material science can be an indication, that there is still a potential to be extracted from electro-active materials by a novel actuator and motor designs [38,39].

The two most common classification methods of piezoelectric motors are based on either the vibration type generated by the inverse piezoelectric phenomenon, or the output motion produced by a motor (Fig. 1, [40]).

In literature and in the industry the classification based on resonant and non-resonant vibration types has been utilized most frequently [51–54]. The widest group of piezoelectric motors in terms of vibration generation is resonant or ultrasonic motors. The ultrasonic motor can be defined by the phenomenon in which electrical energy is converted by the inverse piezoelectric effect to obtain displacement of an actuator at one of its resonant frequencies in the ultrasonic range. This microscopic vibration is then amplified by means of friction or contact-less coupling with a moving element of the motor [55–58].

This work aims to review recent advancements in the field of piezoelectric ultrasonic motors and to categorize them in terms of the macroscopic output motion generated, namely rotary and linear - single degree-of-freedom (DOF), spherical, rotary-linear and planar, which are multi-DOF designs.

The authors focused mostly on research articles published in the last five years. However, the authors made a few exceptions to highlight a unique concept. Search criteria were as follows:

- The article written in English appeared in a journal in the last five years (from 2015 to 2020).
- The primary subject of the article was the development of piezoelectric ultrasonic motors which included analytical, numerical and experimental analysis.

* Corresponding author.
E-mail addresses: roland.ryndzionek@pg.edu.pl (R. Ryndzionek), lukasz.sienkiewicz@pg.edu.pl (Ł. Sienkiewicz).

https://doi.org/10.1016/j.ultras.2021.106471
Received 23 October 2020; Received in revised form 17 May 2021; Accepted 17 May 2021
Available online 28 May 2021

- The measurement data should contain resonant frequencies, speed-torque characteristics for rotary motors, thrust for linear motors and speeds for each axis in the case of multi-DOF designs.

Articles that did not present experimental analysis were excluded from the review. With such criteria the search was executed in Scopus and IEEE Explore databases. Title, abstract and keywords were analyzed for the string:(”linear/rotary/spherical/ planar/rotary-linear” AND ”ultrasonic” AND ”motor”).

After removing duplicates, analysing if the titles and abstracts fulfil the research criteria, the authors examined the full manuscripts. The Scopus database returned 261 records between 2015 and 2020, while 121 items were found in IEEE Explore for the same period. The most represented sub-group were rotary and linear motors, namely single DOF designs. The spherical, cylindrical or planar motors representing the multi-DOF sub-group were noticeably less frequently investigated (Fig. 2).

This review is organised into five chapters which describe the main sub-groups of ultrasonic motors (USM). Chapter 2 is dedicated to rotary ultrasonic motors (RUSM), which are divided into traveling wave (TWUSM), standing wave (SWUSM) and bending mode ultrasonic motors (BUSM). Linear ultrasonic motors (LUSM) are presented in Chapter 3. The next chapter deals with multi-DOF designs, such as spherical ultrasonic motors (SUSM) described in sub-chapter 4.1, rotary-linear ultrasonic motors (RLUSM) - in sub-chapter 4.2 and planar ultrasonic

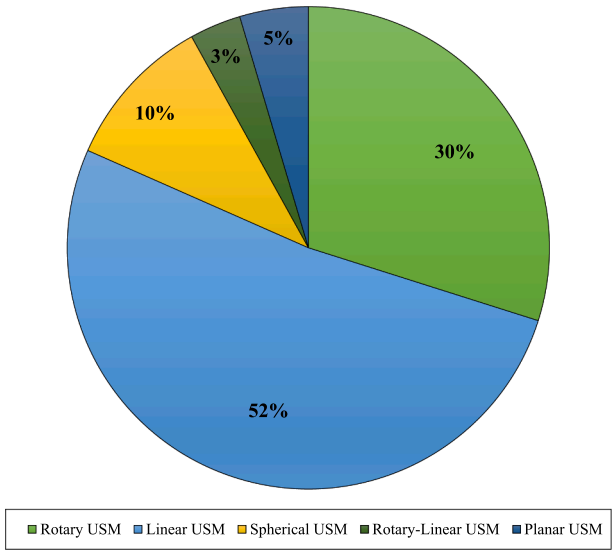

Fig. 2. Percentage division of ultrasonic motor designs with respect to the macroscopic movement generated by the motor, according to the Scopus database for years 2015–2020.

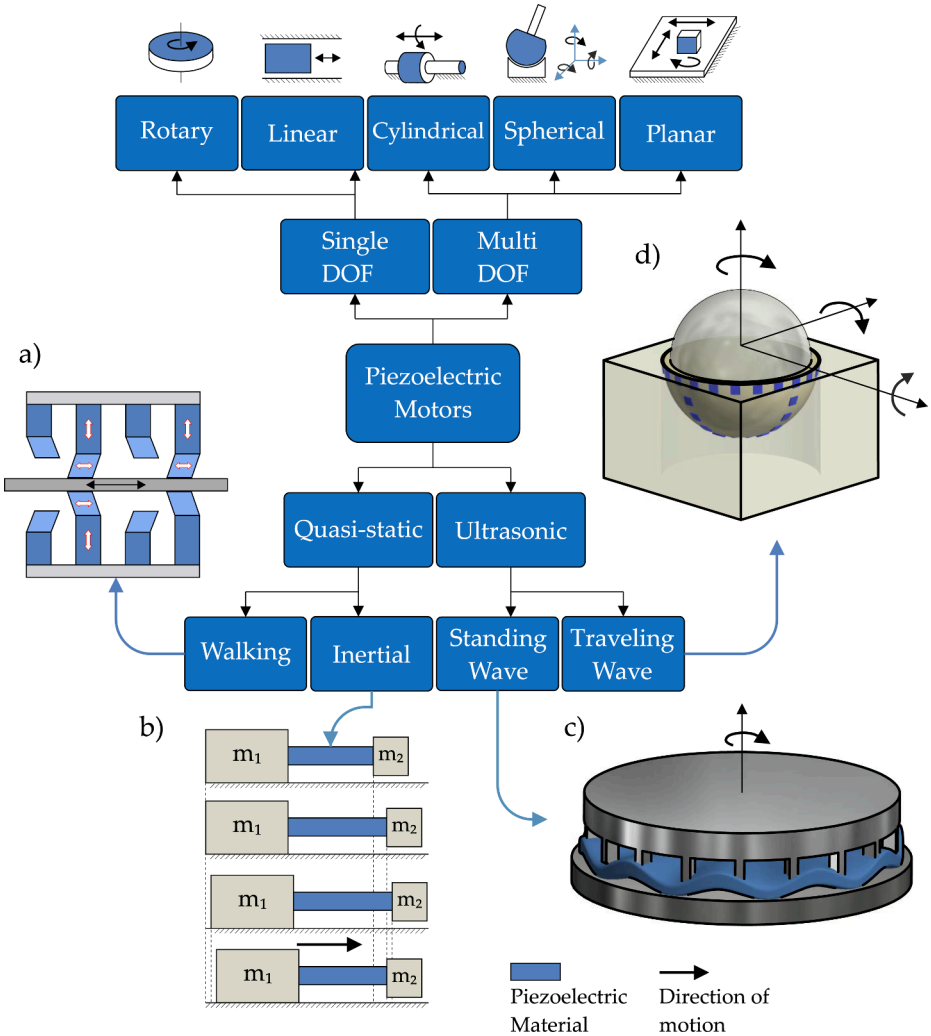

Fig. 1. A classification of piezoelectric motors according to vibration types and to output motion [40]: (a) walking linear motor [41–43]; (b) inertial linear motor [44–46]; (c) standing wave rotary motor [47,48]; (d) traveling wave spherical motor [49,50].

motors (PUSM) - in sub-chapter 4.3. The selected electro-mechanical and geometrical motor parameters are presented in tables in the corresponding chapters. In the final chapter, the authors give their opinion on the present state of USM and list possible challenges and perspectives for future ultrasonic motors.

2. Rotary ultrasonic motors

An ultrasonic motor is a drive system that uses a mechanical vibration in the ultrasonic wave range as its driving source. The principle of operation of these systems is based on the activity of a resonant mode of a mechanical structure to generate a kinematic interface and to transform micro travel movements into motion of large amplitude.

Most of the designs use the PZT ceramics to generate the vibrations [59,60]. In general, the piezoelectric motors are composed of four main parts: stator, rotor, piezoelectric ceramics, and a dedicated power supply. Despite the relatively simple mechanical design, there is a variety of structures that produce rotary motion [61,62]. Table 1 illustrates the mechanical output performances of some existing rotary ultrasonic motors in the last few years.

2.1. Traveling and standing wave ultrasonic motors

The most common group among the rotary ultrasonic motors (among the ultrasonic motors, as well) is traveling wave ultrasonic motors (TWUSM). Consisting of a ring shape stator and driving tips, this structure is similar to a Shinsei motor [63] designed in 1986 [64–66]. The TWUSM have been applied successfully in the manipulators and nano-positioning systems due to their high resolutions (e.g. camera focus system [67,68]). The principle of operation of the TWUSM is based on traveling wave generation by the piezoelectric ceramic assembly which is supplied by two sinusoidal, phase-shifted voltages [69–72] (Fig. 3a). The direction of elliptic motion generated by the ceramics is the opposite to the direction in which a traveling wave propagates (Fig. 3a) [73]. However, friction loss between the stator and the rotor, dielectric loss of the piezoelectric materials and mechanical damping loss of the stator are the heat sources. Thus, they generate significant heat and cause the temperature rise of the motor [74].

A structure described (Fig. 3b) by Xuefeng Ma et al. in [77] has reduced numbers of PZT ceramics (from 128 in the first prototype to 16). A real novelty comes with the PZT ceramics orientation and the polarization which is perpendicular to the stator. The dimensions of the motor are as follows: external diameter - 60 mm, thickness of the stator around 15 mm. For a supplied voltage of 400 Vp-p at 24.86 kHz the motor rotational speed is 52.45 rpm.

Table 1
Performances of chosen existing ultrasonic rotary piezoelectric motors.

Reference	Year	Frequency [kHz]	Speed [rpm]	Torque [mNm]
X. Ma et al. [77]	2020	24.86	52.45	30
L. Yang et al. [95]	2020	55.86	405	20
D. Bai et al. [83]	2019	20.86	342	72
C. Jiang et al. [82]	2019	74.0	45	400
L. Wang et al. [15]	2019	77.3	2200	0.5
L. Wang et al. [80]	2018	50.1	7000	0.5
R. Ryndzionek et al. [96]	2018	24.4	62	400
P. Hareesh et al. [97]	2018	54	30	0.5
V. Dabbagh et al. [98]	2017	49.6	122	0.32
D. Xu et al. [99]	2016	40.5	64	10.4
X. Ynag et al. [92]	2016	57.47	342	6.26
Y. Zhao et al. [79]	2016	39.5	2000	0.37
Y. Ma et al. [51]	2016	44.8	80	2
Y. Liu et al. [100]	2016	21.5	158	53
T. Peng et al. [101]	2015	20	147	22.5
W. Chen et al. [78]	2014	19.85	146	1000
Y. Liu et al. [94]	2013	25.1	298	9300

A next structure has been presented by Weishan Chen et al. in [78]. This motor uses 20 PZT stacks with opposite polarization nested alternately into the stator slots (Fig. 3c).

The structure is symmetrical and uses two rotors to improve the mechanical output characteristics. The main dimensions of the motor are: external diameter of the stator - 60 mm, thickness of the stator - 15 mm, thickness of the full structure 67 mm. The motor resonant frequency is 19.85 kHz. With 150 Vp-p supplied to the ceramics, this motor obtained maximal speed of 146 rpm.

Although, rotational speeds in the range of low hundreds of rpms are more common, rotary ultrasonic motors may reach very high rotational speeds. This has been proven by Yanqiang Zhao et al. The authors developed an oblate-type ultrasonic micro-motor with multi-layer piezoelectric ceramic and chamfered driving tips [79]. The motor consists of a stator, a rotor, and shells (Fig. 4) and and has impressive micro-scale dimensions. Moreover, the stator is fabricated with a multilayer piezoelectric ceramic glued to a copper ring with six driving tips. In experimental tests, micro-motor reached 2100 rpm and 0.3 mNm at the voltage of 20 Vp-p and frequency of 35.5 kHz. Since then, even higher speed designs were proposed, reaching 7000 rpms at the drive voltage of 350 Vp-p and a motor with external dimensions of 29x9 mm [80].

The smaller subset of rotary ultrasonic motors is represented by the standing wave ultrasonic motor (SWUSM). The standing wave ultrasonic motor needs only one vibration mode excited by a single-phase sinusoidal voltage. Standing waves are produced whenever two waves of identical frequency interfere with one another. The stator/rotor contact is discontinuous, characterized by fixed points along the contact surface. In contrast to the TWUSMs, where the contact is constant, and the rotor moves along with the traveling wave.

A radial standing wave ultrasonic motor has been presented in Fig. 5a and was designed by Xiaoxiao Dong in [81] and Chunrong Jiang et al. [82].

The principle of operation is based on utilizing the first-order radial vibration mode of the stator. The main part of the motor is stator, comprising of the PZT ceramics, the metal ring and the leaf springs (Fig. 5b). The motor has been manufactured and the continuous contact behavior between the stator and rotor is confirmed by contact test results. The normal drive frequency of the stator is 74 kHz with rotary speed of 45 rpm and blocking torque of 0.4 Nm. This prototype is an example of micro-meter motor with the external diameter of the structure reaching 30 mm. In the further research the authors are declaring to focus on the improvement of the model of the interaction between the load and stator vibration.

The motor developed by Bai Deen et al. [83] and presented in Fig. 6a has an interesting design. The motor consists of a leftward bending longitudinal-torsional convertor, and a rightward bending longitudinal-torsional convertor (stator), piezoelectric stack, rotor, and screws. Moreover, the convertor (stator) has driving tips with a specific shape (Fig. 6b). Those tips amplify the vibrations produced by the piezoelectric ceramics.

A variety of experimental tests were conducted by authors. The optimum excitation frequency of the actuator for pushing the rotors was 20.86 kHz. The prototype obtained a peak no-load speed of 342 rpm. Furthermore, the maximum torque of 72 mNm was achieved at the speed of 60 rpm.

2.2. Bending mode ultrasonic motors

The third group of ultrasonic motors uses a bending mode of vibration to create macroscopic rotary motion [84,85]. On one hand, bending mode ultrasonic motors (BUSM) have a simpler structure which is favorable in terms of industrial application. On the other hand, such mechanical construction results in less stable contact conditions (a single point of contact). The BUSMs typically consist of a stator, rotor, piezoelectric ceramics, and a shaft [86–90], resembling the usual build of other rotary ultrasonic motors. The difference is in the exciting mode

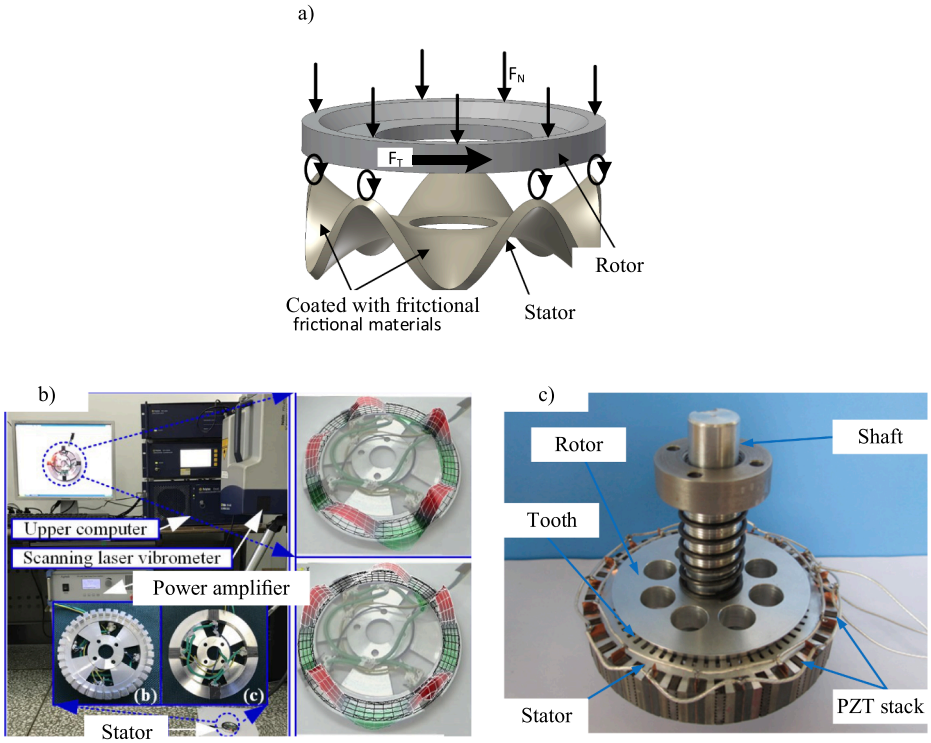

Fig. 3. a) A principle of operation for a TWUSM [75,76]. A rotary traveling wave ultrasonic motor presented in b) Xuefeng Ma et al." © 2021 IEEE. Reprinted, with permission from [77]" and c) Weishan Chen et al." © 2021 IEEE. Reprinted, with permission from [78]".

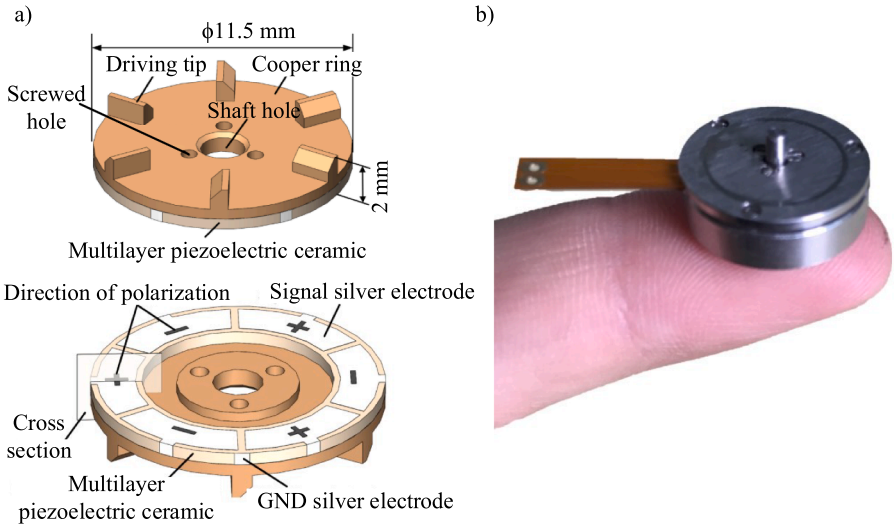

Fig. 4. (a) The ultrasonic micro-motor stator structure, front and back view. (b) The manufactured prototype of micro-motor. "Reprinted from [79], with the permission of A.IP Publishing.".

of piezoelectric ceramics - the bending mode of the stator is used. In general, the stator consist of two cylindrical blocks with a piezoelectric ceramics placed between them (Fig. 7) [91].

Xiaohui Yang et al. in [92] have presented an evolution of their research (Fig. 8a). A cylindrical ultrasonic motor using a longitudinal-bending hybrid vibrations has been developed. This is an improved version of the cylindrical motor described in [93]. A new design requires only two pieces of PZT ceramics instead of four pieces. The operating principle of the motor employs two basic vibration modes, which are the first longitudinal mode and the third bending mode of the beam. The stator consists of a metal beam, cylinder, and two ceramic plates. Moreover, the cylinder and beam have been manufactured from the same block of aluminum.

In laboratory tests the authors obtained a maximum speed of 42 rpm and a maximum output torque of 6.26 mNm with drive voltage and frequency of 100 Vp-p and 57.47 kHz, respectively.

Another original structure has been developed by Yingxiang Liu in [94]. This rotary piezoelectric motor utilizes multi-bending vibrators (Fig. 8b). The purpose of this design was to achieve a high output power. The presented motor has four bending vibrators which are set around the circumference of the rotors. Moreover, due to the symmetrical structure, utilization of two rotors is possible. Each vibrator is equipped

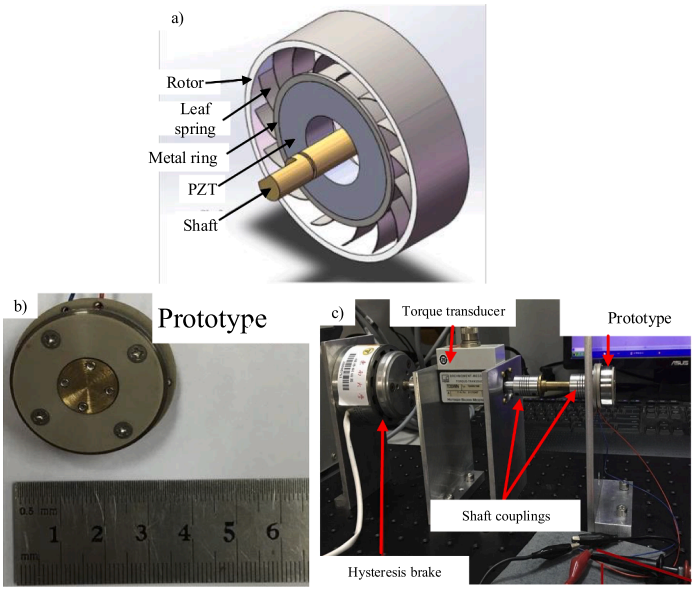

Fig. 5. a) Configuration of the radial standing wave ultrasonic motor b) The ultrasonic micro-motor stator structure, front and back view. c) The manufactured prototype of micro-motor [81,82]. "Reprinted, with permission. from Elsevier".

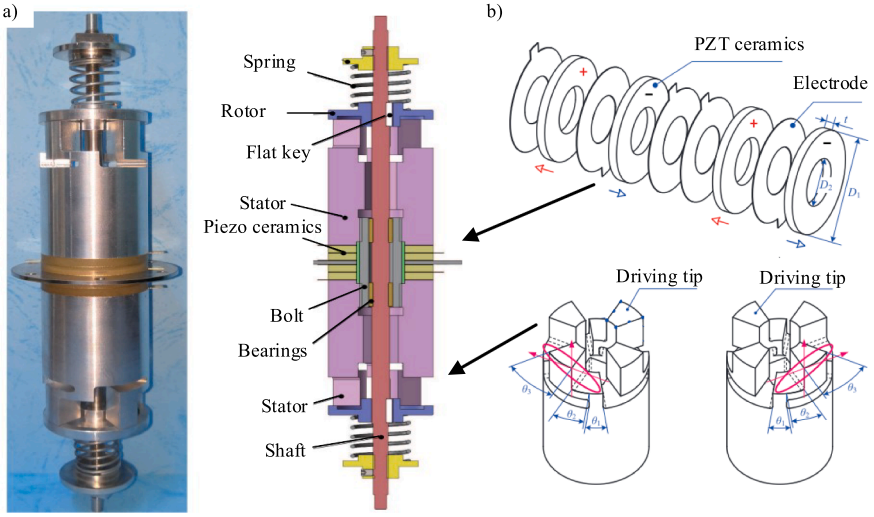

Fig. 6. a) The manufactured prototype; b) a cross-section of a motor developed by Deen Bai et al."© 2021 IEEE. Reprinted, with permission from [83].".

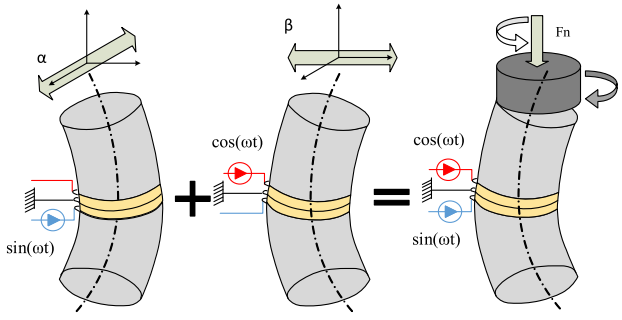

Fig. 7. A principle of operation for a bending mode ultrasonic motor.

with two groups of PZT elements (PZT-A and PZT-B). The multi-bending feature of the vibrators is due to the different voltage signals thus different bending modes. PZT-A and PZT-B can excite the flexural bending mode of vibration in the circumferential direction of the rotor and the radial direction of the rotor, respectively. The prototype has been set under experimental investigation and mechanical characteristics have been verified. The working frequency was from 22.0 kHz to 28.0 kHz with drive voltage of 200 Vp-p. In this case the maximum speed was 301 rpm. The maximum achieved torque was 9.2 Nm, which is indeed an impressive result for an ultrasonic motor.

With 30% of total USM proposed in the considered period, rotary ultrasonic motors are the second largest group among the USM designs. Moreover, it is the most widely recognized type of piezoelectric ultrasonic motor, arguably thanks to TWUSM concept introduced in the 1970s and commercialized in the 1980s. Modern applications of RUSMs include high precision positioning stages evaluated for space or drive elements in high-end distance and angle measurement stations [102,103]. The performances of some existing RUSMs are presented in Table 1 and Table 2. The listed values were extracted directly, or they were assessed based on geometry provided in the references. Modern rotary USM can achieve impressive mechanical characteristics, with maximal speed up to 7000 rpms and torque up to 9.2 Nm. With

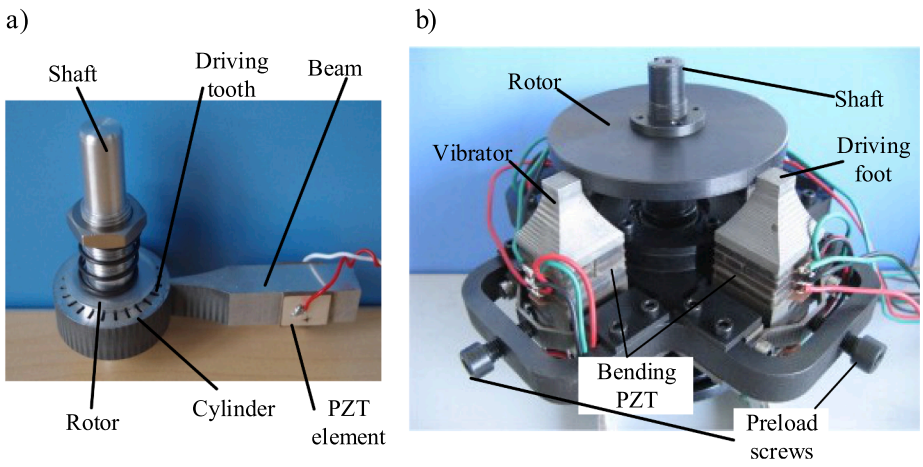

Fig. 8. a) Longitudinal-bending hybrid USM proposed by Xiaohui Yang et al.[92]. "Reprinted, with permission from Elsevier". b) BUSM proposed by Yingxiang Liu [94]. "Reprinted, with permission from Elsevier.".

Table 2
Performances of chosen existing ultrasonic rotary piezoelectric motors - continued.

Reference	Power density [W/kg]	Torque density [Nm/kg]	Torque/ Volume [Nm/m^3]	Volume [m^3]	Weight [kg]
[77]	2	3.67			3.00E-2
[95]			4.63E + 3	4.32E-6	
[83]			5.87E + 2	1.23E-4	
[82]			3.83E + 4	1.05E-5	
[15]	9.72	0.14	7.96E + 1	6.28E-6	3.60E-3
[80]		0.04	9.46E + 1	5.28E-6	1.30E-2
[96]		0.80	2.83E + 3	1.41E-4	5.00E-1
[97]		0.01	6.62E + 4	7.55E-9	5.00E-2
[98]			2.33E + 2	1.37E-6	
[99]	15.6	2.08	6.47E + 3	1.61E-6	5.00E-3
[92]	2.38	0.27	8.04E + 2	7.79E-6	2.35E-2
[79]			6.72E + 2	5.51E-7	
[51]			2.28E + 4	8.78E-8	
[100]	18.99	3.35	1.23E + 4	4.30E-6	1.58E-2
[78]	28.89	5.56	1.05E + 4	9.54E-5	1.8E-1
[94]			3.50E + 4	2.66E-4	

dimensions of the active parts in the micro-meter range, rotary USMs present elevated torque and power density compared to traditional motors designs.

3. Linear ultrasonic motors

In general, a linear ultrasonic motor (LUSM) is a structure that can realize a bidirectional motion by utilizing two separate vibration sources with a phase difference or two superimposed vibrations from one source on the stator [104–106]. Compared with the electromagnetic motor, LUSM has many advantages e.g. high thrust at low speed, structure without reduction gears or low noise operation [107–113]. The basic LUSM design can be realized as a very simple structure, composed only of a stator and a mover. In particular, the stator incorporates a piezoelectric material and a mover is realized as a slider [114,115]. Table 3 presents the mechanical output performances of some existing linear ultrasonic motors.

The first structure that should be introduced is a bimodal standing wave ultrasonic motor developed by Xiang Li et al. [116]. Extended research of the motor has been presented in [117]. A dynamic model taking into account nonlinearities of piezoelectric transducers under high drive voltages is considered. The authors are continuing their research and study on LUSMs [118]. The prototype is presented in Fig. 9 and is composed of a stator with eight PZT-8 piezoelectric patches which

Table 3
Performances of chosen existing linear piezoelectric ultrasonic motors.

Reference	Year	Frequency [kHz]	Speed [m/s]	Thrust [N]
R. Niu et al. [125]	2020	26.60	0.140	3.6
J. Niu et al. [122]	2020	54.34	1.47	96
Y. Tanoue et al. [126]	2020	84.73	0.148	0.29
X. Li et al. [116]	2020	39.5	0.75	ND
Z. Yin et al. [127]	2020	20.1	0.19	10
L. Wang et al. [128]	2018	46.95	0.140	2.8
J. Liu et al. [124]	2018	24.15	0.827	27
S. Shao et al. [120]	2016	24.43	0.83	56
J. Yan et al. [129]	2016	31.12	0.735	1.1
Z. Liu et al. [104]	2016	24.4	0.385	40
X. Li et al. [123]	2015	174	0.23	0.3

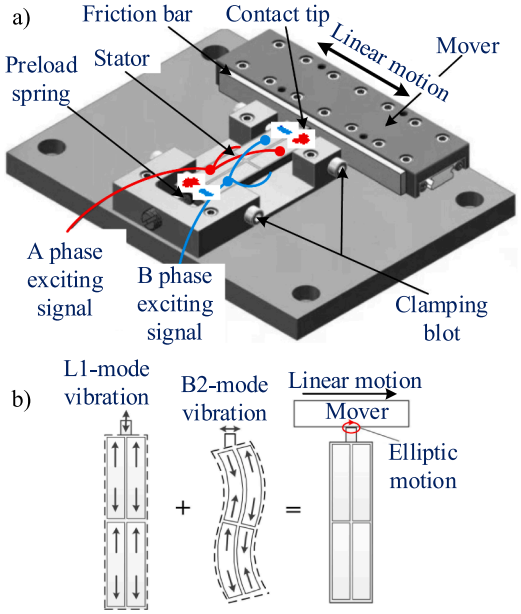

Fig. 9. a) The structure of the proposed motor by Xing Li et al. [116,117], b) Cross-section of the actuator and direction of the vibrations. "Reprinted, with permission .from Elsevier.".

are bonded symmetrically onto a contact tip and a bar. The performance of the prototype is analyzed under different voltage levels from 50 Vp-p to 400 Vp-p (Fig. 10). The maximum measured no-load speed was 0.8

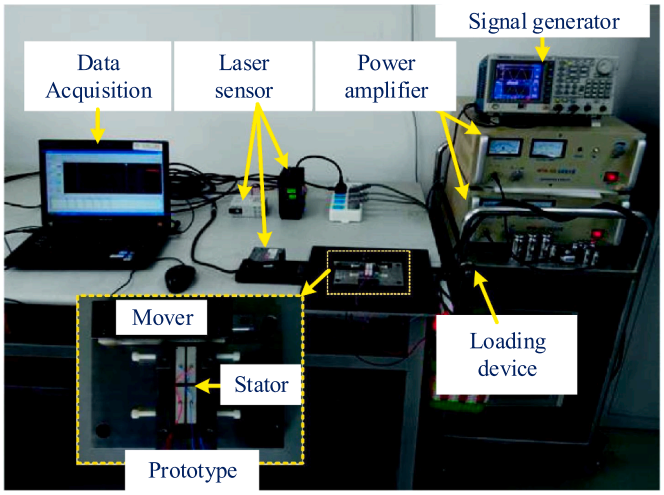

Fig. 10. The manufactured prototype under test of Xing Li et al. [116,117]. "Reprinted, with permission .from Elsevier.".

m/s (at drive voltage of 400 Vp-p and resonant frequency of 39.5 kHz). The application field of this prototype is listed as a precision positioning due to the high step resolution.

Similar structure of LUSM presented in [119] by Shaopeng He et al. is dedicated to deep-sea applications. However, this motor design uses only four piezoelectric ceramics which in combination with the aluminum plate forms a stator. The stator is symmetrical on the xoy and yoz axes (Fig. 11). The ceramics are divided into two groups with opposite polarization directions in each group. During the simulation analysis, authors investigated the influence of water pressure on the resonant frequency and called it a wet modal analysis. However, the results of the analysis showed that pressure of water has little effect on the resonant frequencies. The prototype (Fig. 12) has been tested in submerged state which, as predicted, lowered its performance. The measured velocity of LUSM was 214 mm/s at the drive voltage and frequency of 200 V and 72 kHz, respectively, while the water pressure was 8 MPa.

Some linear ultrasonic motor designs exhibit large output thrust along with the favorable speed. Such an example is a motor (Fig. 13) developed by Shao Sijia et al. presented in [120]. The typical no-load speed and maximum output thrust of the prototype are 0.83 m/s and 56 N under applied voltage of 150 Vrms. However, this optimized design was first reported in 2010 [121].

Another high-powered and high-thrust LUSM is the structure designed (Fig. 14) by Jianye Niu et al. in [122]. The authors reported the maximal thrust force around 96.1 N and no-load sliding speed of 1470

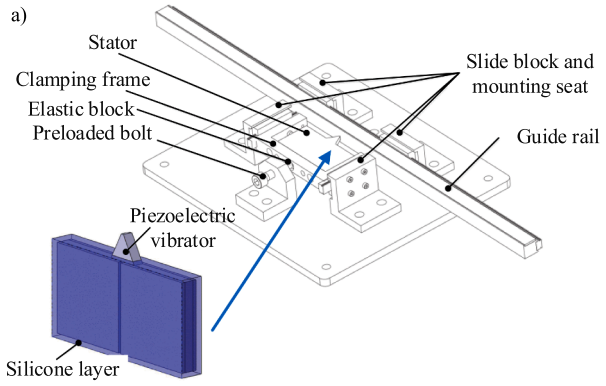

Fig. 11. The structure of the motor proposed by Shaopeng He et al. "©2021 IEEE. Reprinted, with permission from [119].".

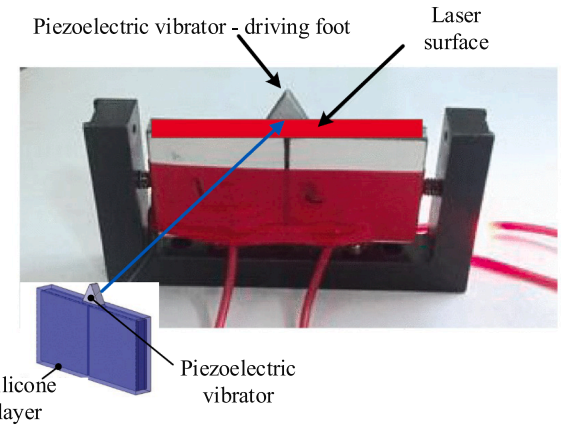

Fig. 12. The prototype of the motor proposed by Shaopeng He et al. "© 2021 IEEE. Reprinted, with permission from [119].".

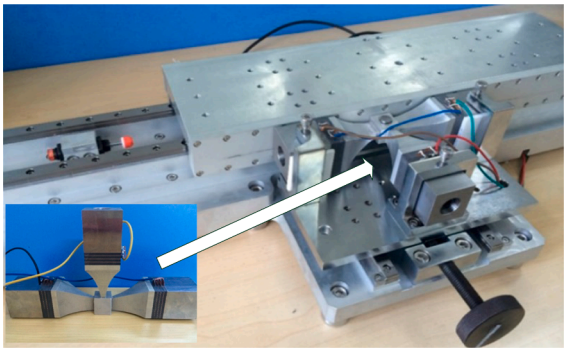

Fig. 13. The structure of the motor proposed by Shao Sijia [120].

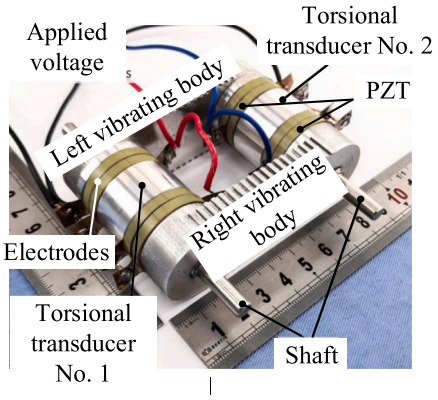

Fig. 14. The structures of LUSMs developed by Jianye Niu in [122].

mm/s. The force and power density reached 234.1 N/kg and 67.8 W/kg respectively, which are relatively high ratios among conventional LUSMs.

Finally, in Fig. 15, the ultrasonic motor with bidirectional motion is presented. This structure has been developed by Liu Zhen et al. in [104].

The motor is composed of a stator, a slider, a preload device, and a base which makes it a simple and compact construction. The output characteristics of the prototype are as follows: maximal thrust of 4.0 kg, which is 33.3 times its own weight, and maximum no-load speed of 385 mm/s.

Linear ultrasonic motors are the most represented group in this review with 52% of total number of USMs, experiencing constant growth since mid 1980s. This is due to inherit qualities of LUSMs such as: simple

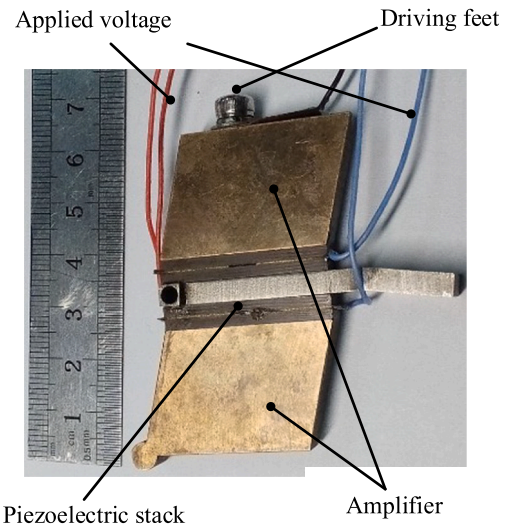

Fig. 15. The novel LUSM driven by a single mode developed by Liu Zhen. "Reprinted from [104], with the permission of AIP Publishing.".

mechanical structure with possibility of adaptation to a given application (various shapes reported in the literature), direct drive with high positioning accuracy and high thrust density. Such features situate LUSMs as a good candidates in the nano-positioning stages (S. Shao et al. [120] - LUSM driving a working platform), miniature machining tools, micro-lens drives in digital cameras (e.g. X. Li et al. [123]), precise biomedical manipulators and robot joints (e.g. J. Liu et al. [124] and S. He et al. [119]). The simple structure of LUSMs sets them as good basis for multi-DOF systems (Table 3). Parameters such as thrust density, weight and size have been presented in Table 4 as a reference point for comparisons.

4. Multi degree of freedom ultrasonic motors

The new functionalities resulting from the simultaneous management of several degrees of freedom within one mechanism (e.g. robotised micro-surgery, micro-positioning for microelectronics or near field microscopy) gave the researchers a particularly rich field of investigation [130–135]. Numerous multi-DOF designs have been reported [136–140] utilizing the principles of traveling and standing waves or combinations of longitudinal ('33'), transversal ('31') and shear modes ('15') described below.

An active element polarized along its length and subjected to a difference of potential applied between two electrodes perpendicular to its polarization axis Ox3 undergoes, by the converse piezoelectric effect, a change in length in the same direction, thus works in mode 33. In a second configuration (mode 31), the element can be polarized in its thickness direction and subjected to an external field oriented in the same direction. Due to transverse coupling, a change in length perpendicular to the polarization direction can be observed. Finally, the application of an electric field perpendicular to the direction of polarization along the axis Ox3 tends to turn the elementary dipoles around the axis Ox2. The resulting deformation can be defined as the shear mode or mode 15. The above clarification is made with the reference axes of the coordinate system marked as Ox3 - z, Ox2 - y and Ox1 - x.

In the following paragraphs, three sub groups of multi-DOF motors are mentioned, namely: Spherical Ultrasonic Motors, which are two or three DOF, Rotary-Linear and Planar Motors - two DOF designs (Table 5).

Table 4
Performances of chosen existing linear piezoelectric ultrasonic motors - continued.

Reference	Weight [kg]	Thrust density [N/kg]	Size [mm]
J. Niu et al. [122]	0.41	234	116 × 91 × 32
Y. Tanoue et al. [126]	0.005	58	20 × 10 × 6
Z. Yin et al. [127]	1.3	7.64	192 × 52 × 52
L. Wang et al. [128]	0.06	46.7	62 × 16 × 16
J. Liu et al. [124]	0.26	103	66 × 58 × 58
S. Shao et al. [120]	24.43	2.3	100 × 100 × 35
J. Yan et al. [129]	0.1	11	83 × 13 × 13
Z. Liu et al. [104]	0.12	440	56 × 50 × 8
X. Li et al. [123]	0.0002	60	5 × 2×2

4.1. Spherical ultrasonic motors

One of the first ultrasonic motors called 'spherical' was the motor developed by S. Toyama in 1991 [141] and later upgraded in [142]. The main purpose of its design was a drive dedicated to the assembling machines, laser cutting or as a single joint in robotics. Nowadays, due to the ongoing progress in the fields of active materials and MEMS technology, many novel, advanced spherical ultrasonic motors (SUSM) are reported.

The first highlighted construction, has been developed by Zhibo Huang, presented in [143] and dedicated to the robot's visual driving systems. The reported motor includes a spherical stator, which utilizes a piezoelectric ceramic spherical shell (Fig. 16a). Moreover, special driving feet, enabling an uniform drive of the rotor, have been placed on the stator. An external rotor formed from two hemisphere shells rotates around X, Y, and Z axes respectively, making it a 3-DOF SUSM (Fig. 16b). The authors prepared the FEA analysis to obtain the resonance frequencies, which are 31.697 kHz, 31.608 kHz, and 32.272 kHz, respectively (Fig. 16c).

The main dimensions of the stator are: sphere outer diameter of the piezoelectric ceramic spherical shell - 30 mm, a diameter of each electrode area - 18 mm, the height of each driving foot - 3 mm and sphere radius of each driving foot - 2 mm. The mechanical output characteristic of the manufactured prototype (Fig. 17) were as follows: the maximum rotary velocity of the rotor around X, Y, and Z axes was 245 rpm, 240 rpm and 318 rpm, respectively. The drive voltage was 140 Vp-p at a frequency of 31.7 kHz.

The second structure worth further examination is a design concept that has been described in [144] by Zheng Li et al. This structure is an impressive, complex motor, which requires high manufacturing precision. In addition, it is an example of an inverted design known from the [138].

Table 5
Performances of chosen existing spherical and rotary-linear piezoelectric ultrasonic motors.

Reference	Year	DOF	Frequency [kHz]	Speed [rpm]	Torque [mNm]
Z. Huang et al. [143]	2020	3	31.73	318	15.3
Z. Li et al. [144]	2020	3	40.35	29	ND
S. Shi et al. [152]	2018	3	54.3	106	17.5
Y. Wang et al. [151]	2018	2	19.98	118	38
J. Yan et al. [153]	2018	3	38.23	327	ND
L. Wang et al. [154]	2018	3	45.2	280	ND
S. Shi et al. [146]	2017	3	26.2	55	118
X. Yang et al. [148]	2016	3	61.2	290	ND
L. Yan et al. [147]	2016	3	446	1519	2.0E-3
J. Wang et al. [155]	2015	2	49.0	92	90

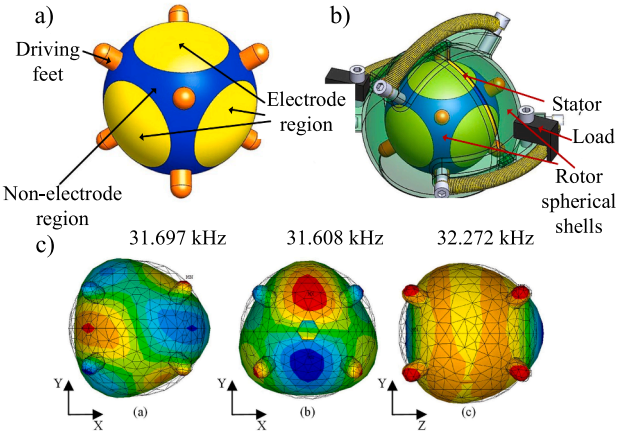

Fig. 16. The structure of a 3-DoF SUSM developed by [143] a) a virtual model of the spherical stator, b) a virtual model of the metal spherical shell rotor, c) Modal analysis results of the proposed motor. "Reprinted, with permission . from Elsevier.".

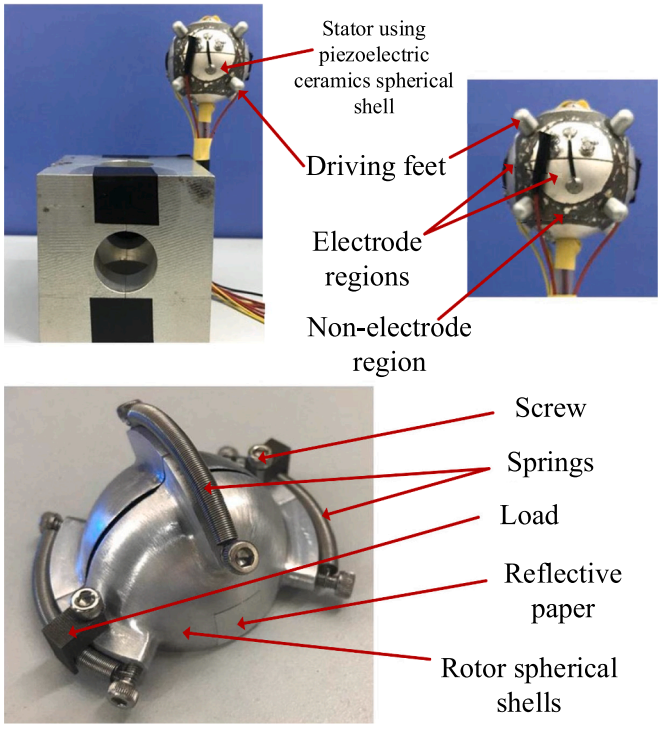

Fig. 17. The structure of a 3-DoF SUSM developed by [143] a full view of the manufactured prototype. "Reprinted, with permission .from Elsevier.".

The structure consists of three stators (Fig. 18a and b) which are placed at an inclined angle of 72.4 degrees in the X-Y plane. A hollow rotor is placed on the stators with the pre-pressure regulator ensuring the stability of the motor. Thus, the 3-DOF movement is available.

The prototype has been tested in laboratory conditions (Fig. 19). The resonance frequency of the motor stator was 40.375 kHz. The series of experiments have been conducted to determine the mechanical output performance. The motor has been tested under different drive frequencies and mechanical output performance was measured in the X-axis, Y-axis and Z-axis. For the frequency of 42.25 kHz the prototype obtained the highest speeds of: 29 rpm, 17 rpm and 16 rpm in the X, Y, and Z axes, respectively. The authors are declaring to gradually miniaturize the motor structure in the future.

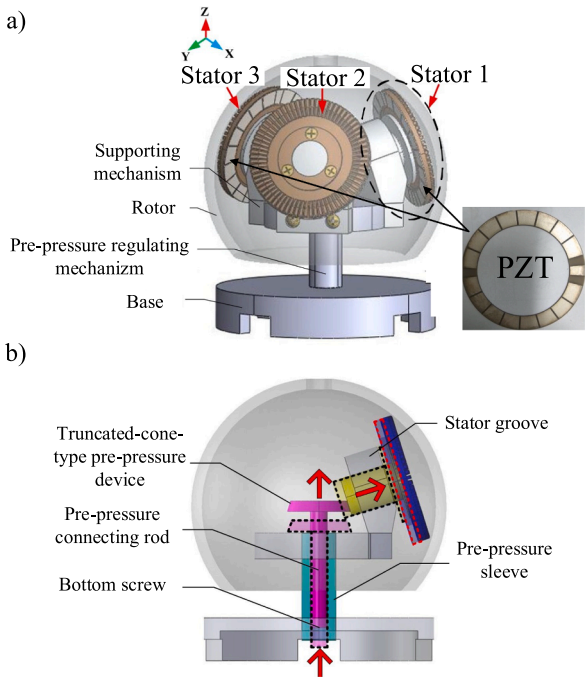

Fig. 18. The structure of a 3-DOF SUSM developed by [144,145] a) a virtual model of the spherical stator, b) a virtual model of the metal spherical shell rotor. "Reprinted, with permission .from Elsevier.".

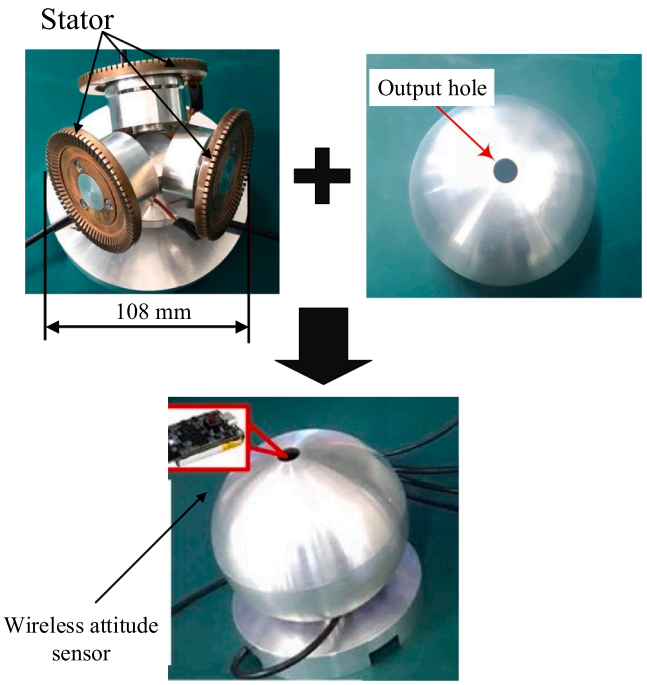

Fig. 19. The full view of the 3-DOF SUSM manufactured prototype by [144,145]. "Reprinted, with permission .from Elsevier.".

Examples of similar 3-DOF SUSMs, often termed as multi-DOF ultrasonic motors are reported [146–148]. These structures have the same spherical, multi-degree rotor and utilize a combination of longitudinal and orthogonal bending vibrations generated in the stator.

In [146], the design by Shi Shengjun et al. uses two sets of PZT ceramics - the inner set and the outer set as shown in Fig. 20a. In total, the motor has 28 pieces of PZT ceramics. The best drive frequency for x, y and z-axis was 26.0 kHz, 26.2 kHz and 26.2 kHz, respectively, while the

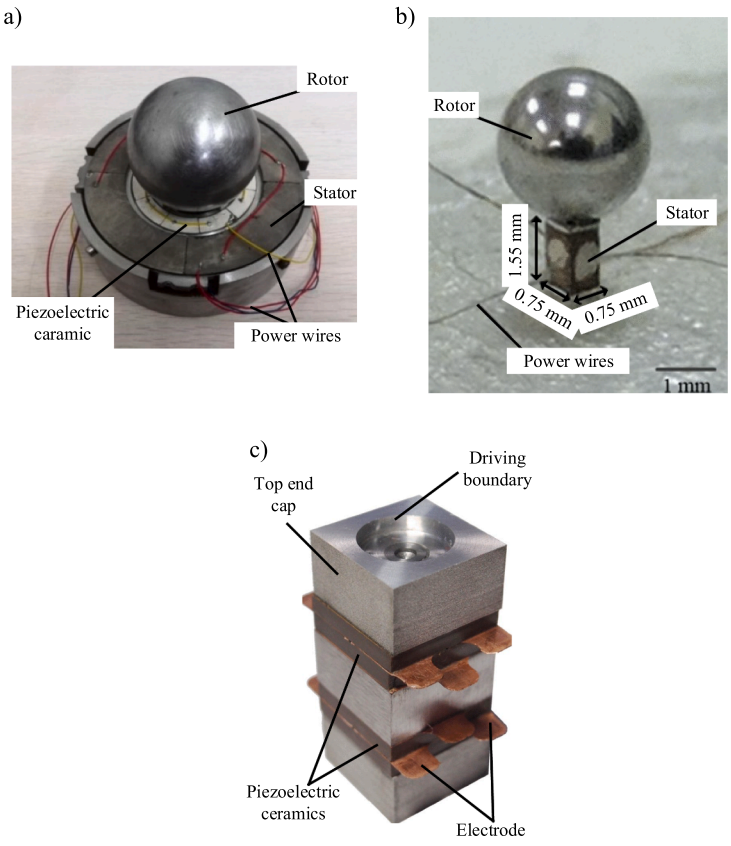

Fig. 20. Chosen structures of SUSMs: a) a ring-type multi-DoF ultrasonic motor design by Shi Shengjun et al. in [146] "Reprinted, with permission from Elsevier", b) micromotor developed by Yan Liang et al. in [149,147] "© 2021 AIP Publishing. Reprinted with permission from [149]", c) a sandwich-type multi-DoF Ultrasonic Motor by Yang Xiaohui et al. "© 2021 IEEE. Reprinted, with permission from [148].".

drive voltage was set to 100 Vp-p. The above drive parameters resulted in the maximum speed for x, y and z-axis of 44, 55, 42 rpm, respectively.

In [147] the 'Compact Traveling Wave Micromotor' has been reported. The motor is characterized by micro dimensions of a stator with a size of 0.75 mm × 1.55 mm. The authors presented a different approach compared to other SUSMs highlighted in this section, utilizing a sandwiched Langevin vibrator as the stator. A cuboid bulk PZT polarized longitudinally occupies the main part of the motor with a metal piece bonded on the top and four copper electrodes, which are attached on the four sides of the PZT. (Fig. 20b). Thus, perpendicular bending modes can be stimulated.

In laboratory tests, this micromotor achieved a no-load speed of 1850 rpm and maximum torque of at least 2 μNm at 60 Vp-p and frequency of 447 kHz. According to authors, the micromotor is still under development stage and should be submitted to further miniaturization.

In [148] a sandwich-type multi-DoF ultrasonic motor with hybrid excitation has been presented (Fig. 20c). It adopts the Langevin type structure but with a square stator's shape. The main motor components are: 3 cubes (a flange bolt and two end-caps) and two pairs of PZT ceramics placed between them. The cube has external dimensions of 20x20x10 mm, while a rotor is a bearing steel ball with 50 mm diameter. The principle of operation is based on a three driving modes which are: the first longitudinal vibration and two orthogonal second bending vibration modes. In combination, they enable the spherical rotor rotation around x, y and z -axis, respectively. The prototype achieved no-load speeds of 109.8 rpm, 107.9 rpm, and 290.8 rpm in the YOZ, XOZ, and XOY driving modes, respectively. The maximum applied voltage was 200 Vp-p at the frequency of 61.7 kHz.

4.2. Rotary-linear ultrasonic motors

In [150], a high-thrust rotary-linear ultrasonic motor (RLUSM) is reported. This design utilizes a three-wavelength exciting mode which is composed of the first and the third bending vibration modes along the axial direction and circumferential direction, respectively. The rotary motion can be converted into linear motion using the screw output shaft, and the torque is converted into linear thrust. The fabricated prototype (Fig. 21) includes three main parts: a metal elastomer, rectangular piezoelectric plates and a screw output shaft. The metal elastomer and twelve rectangular piezoelectric plates constitute the stator, which external dimensions are 36 × 46 mm. The output velocity can reach 0.97 mm/s with the load of 4 N when the peak-to-peak voltage and the excitation frequency are 120 Vp-p and 28.9 kHz. The maximum thrust of the motor is 50.8 N which results in a force density of 247.8 N/kg. Power density and force-volume ratio are 2.94E-3 W/kg and 2.54E + 6 N/m^3, respectively.

Another example of RLUSM is described in [151]. The authors name this structure as a 'Rotary-Percussive Ultrasonic Drill' and design it specifically for rock sampling in Minor Planet Exploration. The drill/motor mainly consists of PZT ceramics, rotary unit, percussive unit, drill tool, and housing, (Fig. 22). Four PZT ceramics are situated in a bolt-clamped structure and placed between rotary unit and percussive unit. Under the drive voltage, PZTs generate longitudinal vibration on both sides. The motor converts one side of longitudinal vibration into rotary motion and the other side into percussive motion. FEA is used to adjust the resonant frequencies of rotary and percussive units to be the same and to ensure an effective drilling performance.

The fabricated prototype includes the following dimensions: drill tool diameter and length is 3 mm and 60 mm, respectively, total length is 270 mm, while the total weight is 590 g. The vibration characteristics

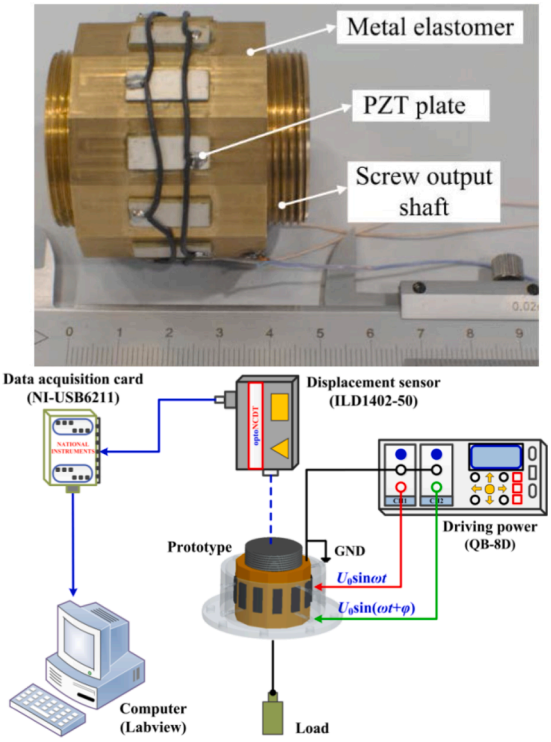

Fig. 21. A structure of a rotary-linear ultrasonic motor: a high-thrust screw-type piezoelectric ultrasonic motor prototype by Hengyu Li et al. in [150] and schematic drawing of the experimental test bench.

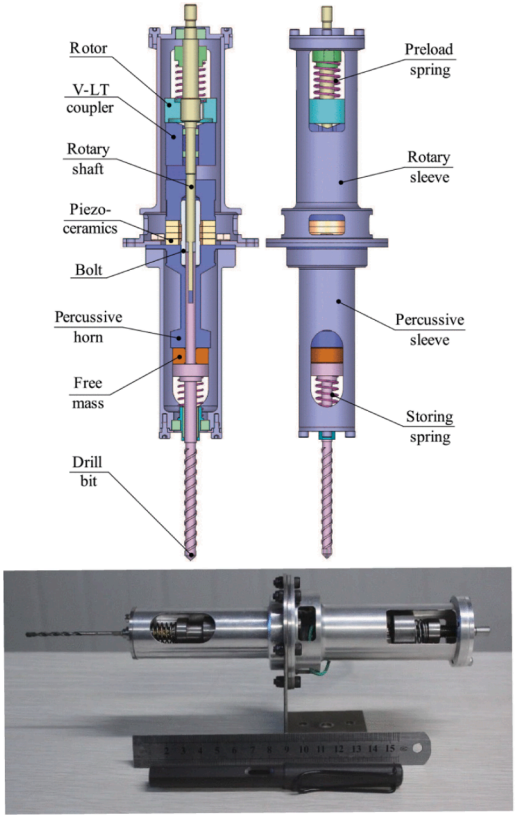

Fig. 22. Rotary-Percussive ultrasonic drill by Wang Yinchao et al. in [151]: CAD drawing and assembled prototype. "© 2021 IEEE. Reprinted, with permission from [151].".

and drilling performance are investigated through tests. Those yield rotary speed of 117.75 rpm and maximum torque of 38 mNm at the preload force of 18 N. Drilling depth of the prototype can reach to 22 mm under the weight on bit of 7 N. The authors aim to improve the drilling capability and to increase the power efficiency in future works.

Chosen electro-mechanical parameters have been presented in Table 5 and Table 6 as reference points for comparisons. Furthermore, spherical and rotary ultrasonic motors have been compared in Fig. 26 located in the following chapter.

4.3. Planar ultrasonic motors

The last subgroup of Multi-DOF USMs is represented by two-DoF motors implementing singular plane movement (Table 7). In general, such structures can also be called planar ultrasonic motors (PUSM). The existing nomenclature of PUSMs is not entirely uniform, hence the authors adopt the simultaneous motion along two axes as a key feature of PUSMs. Nevertheless, this Multi-DOF subgroup is not frequently represented, with only 5% of total USM represented in this work. The majority of piezoelectric planar motors reported in the literature is operating at low frequencies (<100 Hz) [156–162] or single kHz [163,164] and is not considered in this review.

Yingxiang Liu et al. developed a two-DoF planar motor using a longitudinal-bending hybrid sandwich transducer (Fig. 23d). The principle of operation is based on composition of the second longitudinal and fifth bending modes of the motor. The reported prototype is composed of two end caps, two horns, four longitudinal-bending PZT ceramics and eight half-pieces of bending PZT ceramics.

All parts are clamped by a screw (Fig. 23c). The authors measured series resonance frequencies and note the fifth bending vibrations along OZ and OY axis at 22.38 and 22.25 kHz, while the second longitudinal vibration along the OX-axis is 22.13 kHz. The laboratory tests resulted in a maximum no-load velocity in X and Y-directions at 685 and 657 mm/s under voltages of 500 Vp-p, respectively (Fig. 23a and b). Authors claim to focus on its application in a deployable mechanism and dimension optimization in the future.

Another structure is a PUSM designed by Xiangyu Zhou et al. in [166]. This motor utilizes five vibration modes: symmetric and anti-symmetric bending vibration modes of stator in the XOY plane, symmetric and anti-symmetric longitudinal vibration modes of stator along the x-axis and symmetric bending vibration mode in the XOZ plane. The main parts of the motor are: a stator with two Langevin transducers and a pair of isosceles triangular beams, piezoelectric ceramics, electrodes and a screw. The prototype has been manufactured (Fig. 24) and and

Table 6
Performances of chosen existing spherical and rotary-linear piezoelectric ultrasonic motors - continued.

Reference	Torque/ Volume [Nm/m^3]	Power density [W/kg]	Torque density [Nm/kg]	Volume [m^3]	Weight [kg]
Z. Huang et al. [143]	1.23E + 2	ND	ND	1.25E-4	ND
S. Shi et al. [152]	1.01E + 4	ND	ND	1.74E-6	ND
Y. Wang et al. [151]	ND	33.9	0.06	ND	0.59
S. Shi et al. [146]	2.42E + 3	ND	ND	4.88E-5	ND
X. Yang et al. [147]	2.29E + 3	ND	ND	8.72E-10	ND
J. Wang et al. [155]	4.82E + 2	ND	0.17	1.87E + 4	0.544

Table 7
Performances of some existing planar piezoelectric ultrasonic motors.

Reference	Year	Frequency [kHz]	Velocity [mm/s]	Load Force [N]	Force density [N/kg]
Y. Sato et al. [167]	2020	81.5	ND	0.5	ND
Y. Liu et al. [165]	2019	22.3	685	14	15.4
X. Zhou et al. [166]	2016	35.5	211.3	3.15	70
Z. Chen et al. [168]	2014	86.3	35	0.25	251

tested.

The resonance frequencies have been measured in all vibration modes: symmetric bending mode and anti-symmetric bending mode in the XOY plane, symmetric longitudinal mode and anti-symmetric longitudinal mode along the x-axis and symmetric bending mode in the XOZ plane were 37.04, 36.51, 65.71, 64.36 and 34.98 kHz, respectively. Finally, the mechanical output parameters have been tested. The maximum no-load speed was 211.3 mm/s under the drive frequency of 35.45 kHz and voltage of 400 Vp-p.

In this section chosen multi-DOF ultrasonic motors have been described. This subgroup of USM represents 18% of motors considered in this review, with spherical designs being the most represented multi-DOF subset in the examined period (Fig. 2). Embedding more degrees-of-freedom into a single motor is a major way of building size-efficient systems, because reducing the number of actuators lowers the required space and weight while it does not limit functionality. Therefore, modern multi-DOF USMs are popular in applications, where requirements of high resolution along with restrictions on weight and volume are excluding other types of motors. Those include, but are not limited to: micro-scale machining tools, surgical manipulators, automatic visual driving systems, haptic interfaces and nano-precision motion stages. Several authors report extreme environments applications such as: extraterrestrial or deep-sea exploration.

5. Conclusion and outlook

In this work, a comprehensive review of resonant ultrasonic piezoelectric motors is provided. This review classifies the existing resonant type piezoelectric ultrasonic motors into four groups in terms of their macroscopic output motion. Those are: Rotary Ultrasonic Motors (RUSM), Linear Ultrasonic Motors (LUSM), Spherical Ultrasonic Motors (SUSM), Rotary-Linear Ultrasonic Motors (RLUSM) and Planar Ultrasonic Motors (PUSM). A total of 261 papers dealing with piezoelectric ultrasonic motors have been published in various research journals since 2015. The average number of papers per year is 43.5 for the reviewed period compared to 57.6 for the first half of the 2010s. A decline in the number of papers published per year can be observed in the Fig. 25. Those values were obtained thanks to the methodology explained in the first chapter. Thus, works issued as a conference materials or articles written in languages other than English were excluded from this review.

LUSMs and RUSMs, are undoubtedly the most widely recognised groups, with the average of over 22 and 13 papers per year, respectively. On one hand, LUSMs and RUSMs are experiencing a less dynamic development during the reviewed time frame, with lower number of R&D reports per year compared to the first and beginning of second decade of the XXI century. While novel and unique designs are still emerging, research activities are less intensive in those subgroups of Ultrasonic Motors. On the other hand, one can observe increased efforts in the field of Multi-DOF Ultrasonic Motors, namely: SUSM, RLUSM and PUSM designs. The authors believe that this can be attributed to ongoing miniaturization and advancements in CNC machining and metal 3D printing techniques as well as developments in the field of ceramics with lower losses and stable piezoelectric coefficients in broader temperature range. Moreover, the functional efficiency of Multi-DOF designs proves itself well in applications where specific motions are required and the drive's volume must be minimized.

The performance of reviewed RUSM and SUSM prototypes can be assessed thanks to a comparison presented in Fig. 26. Similar comparison is provided for LUSMs, RLUSMs and PUSMs in Fig. 27. No-load speeds and stall torque/thrust values found there, together with power densities, torque densities and torque-volume ratios listed in the Tables 2, 4, 6 and 7 indicate how diverse the ultrasonic motors are and how can they compete with more traditional electro-magnetic motors. The

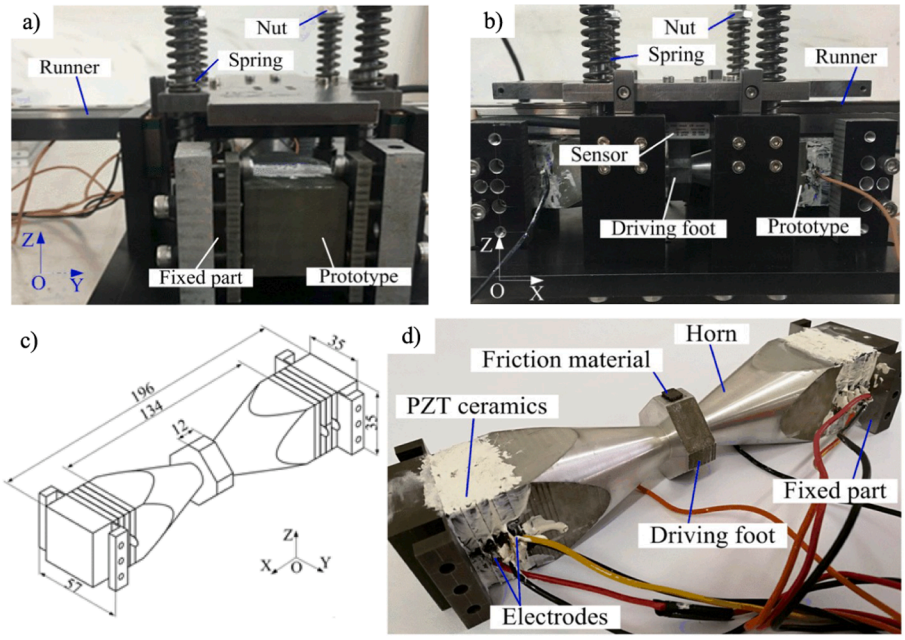

Fig. 23. Prototype of the PUSM presented in [165]: a) Measurements in Y axis, b) Measurements in X axis, c) Prototype's dimensions, d) Manufactured prototype. Figures "© 2021 IEEE. Reprinted, with permission from [165].".

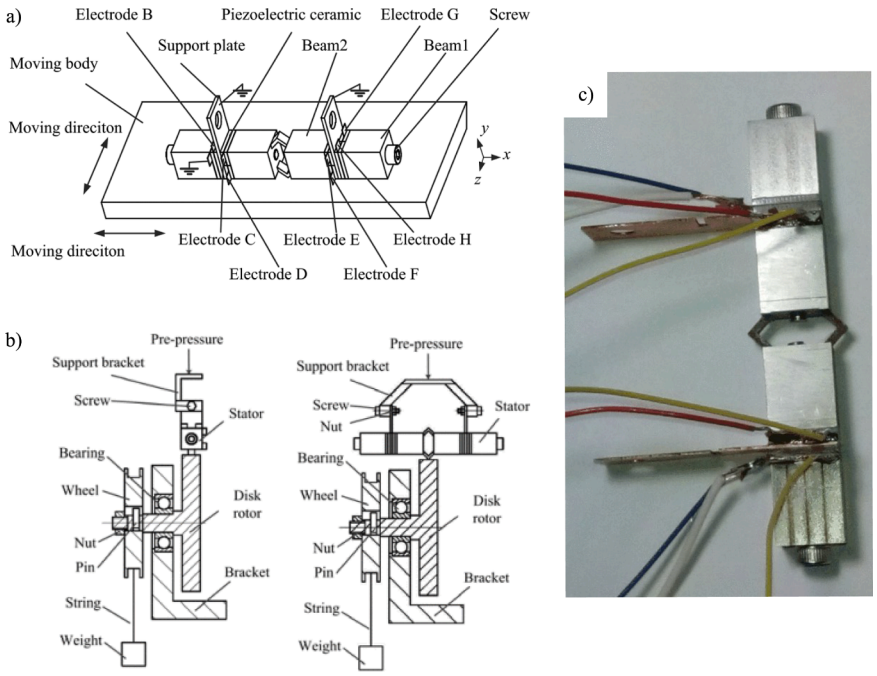

Fig. 24. The structure of PUSM described in [166]: a) The structure of PUSM described in [166], b) Schematic diagram of driving experiment along the X and Y axes, c) prototype of the motor. Figures "© 2021 IEEE. Reprinted, with permission from [166].".

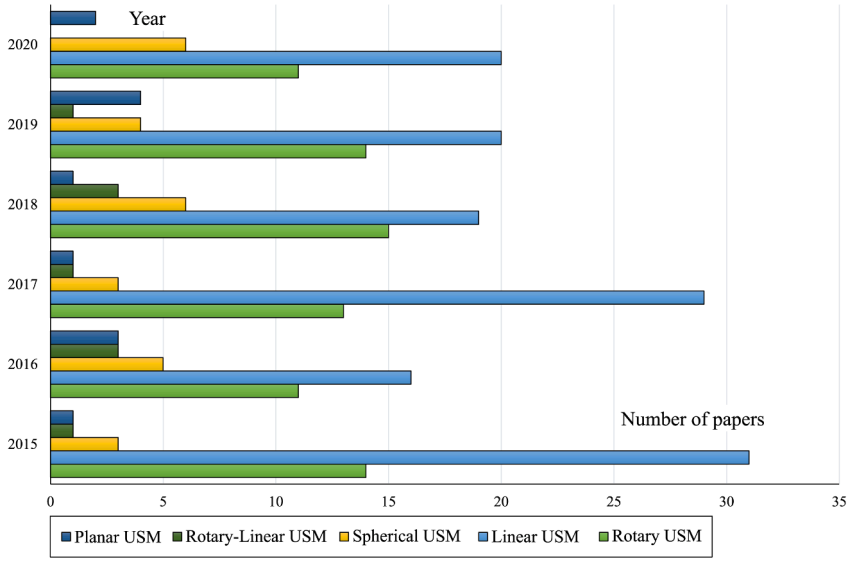

Fig. 25. Number of USM designs per year with respect to the output motion generated. According to the Scopus database for years 2015–2020.

performance of USMs is especially evident in applications requiring mm-size dimensions and weight in the range of single grams.

Several future challenges must be addressed to sustain the interest in USMs in space and volume constrained applications and to reintroduce them to a broader range of use-cases.

The most evident perspectives for USM development are listed as follows.

Improvement of the life cycle. Current USMs operate under the friction coupling between the stationary and the moving parts of the motor. This feature limits the motor's longevity to single tens of thousands of hours. New friction coupling methods as well as optimisation of existing materials and surfaces should be further investigated. Another trend aiming to overcome this challenge is a contact-less design, using near-field acoustic radiation created in the air or fluid between the rotor and the stator [55,169].

Temperature management. The heating of USMs is inherently connected with their low efficiency. Elevated temperature affects the resonant frequencies, even further reduces the efficiency and finally degrades the mechanical output of the motor. Future research activities should focus on further material development, in particular, achieving lower dielectric dissipation and higher mechanical quality factors, while maintaining good electromechanical coupling factors. Another perspective for ensuring favourable resonance conditions is developing new, robust control strategies with drive frequency tracking [170,171].

Simplicity of manufacturing. A great variety of USM structures is reported in the time-frame of this review, yet, many of them are difficult

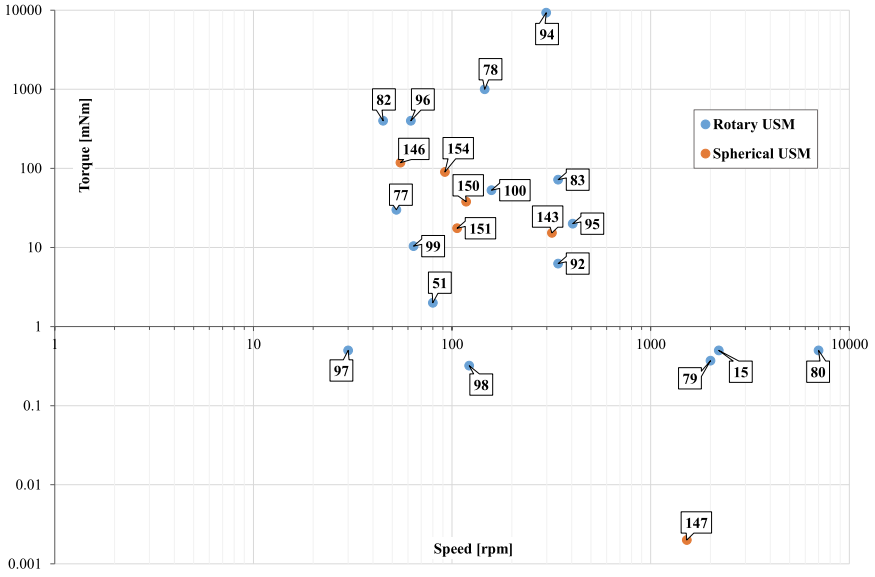

Fig. 26. Comparison of Rotary and Spherical USMs in terms of no-load speed in rpm and stall torque in mNm; Labels indicate the references.

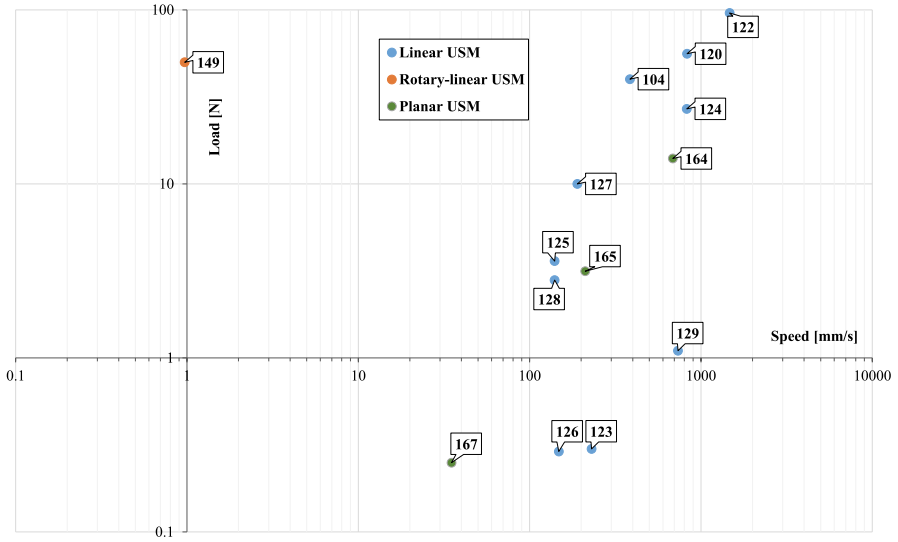

Fig. 27. Comparison of Linear and Planar USMs in terms of no-load speed in mm/s and maximal load in N; Labels indicate the references.

or impractical to manufacture. Instead, a trend to design a simple motor with fewer number of parts should be generally adopted. Modern fabrication methods such as additive ultrasonic manufacturing from metal foils can aid with the simpler motor assembly, increase the repeatability and reliability, improving the functionality and efficiency of novel ultrasonic motors.

The piezoelectric ultrasonic motors are present roughly for 50 years, and there is a visible decline in the interest in USMs compared with the previous decades. However, novel or perfected designs are still emerging. This fact can be attributed to trends existing in the industry, e. g. ongoing miniaturisation and growing need for functional efficiency. From a critical point of view, USMs may not ever be reintroduced commercially on a larger scale.

The R&D effort will continue, nevertheless, aimed at specific applications. In the author's opinion, those use cases imposing considerable limitations on size and volume, while requiring high functionality remain the niche for ultrasonic motors.

Declaration of Competing Interest

The authors declare that they have no known competing financial interests or personal relationships that could have appeared to influence the work reported in this paper.

References

[1] K. Uchino, Piezoelectric ultrasonic motors: overview, Smart Mater. Struct. 7 (3) (1998) 273–285, https://doi.org/10.1088/0964-1726/7/3/002.
[2] J. Wallaschek, Piezoelectric Ultrasonic Motors, J. Intell. Mater. Syst. Struct. 6 (1) (1995) 71–83, https://doi.org/10.1177/1045389X9500600110, http://journals.sagepub.com/doi/10.1177/1045389X9500600110.
[3] H. Hirata, S. Ueha, Design of a Traveling Wave Type Ultrasonic Motor, IEEE Trans. Ultrason. Ferroelectr. Freq. Control 42 (2) (1995) 225–231, https://doi.org/10.1109/58.365236.
[4] N.W. Hagood, A.J. McFarland, Modeling of a Piezoelectric Rotary Ultrasonic Motor, IEEE Trans. Ultrason. Ferroelectr. Freq. Control 42 (2) (1995) 210–224, https://doi.org/10.1109/58.365235.

[5] A.M. Flynn, D.J. Ehrlich, D.J. Ehrlich, D.J. Ehrlich, D.J. Ehrlich, R.A. Brooks, L. E. Cross, L.S. Tavrow, S.F. Bart, K.R. Udayakumar, Piezoelectric micromotors for microrobots, J. Microelectromechanical Syst. 1 (1) (1992) 44–51, https://doi.org/10.1109/84.128055.
[6] K. Spanner, B. Koc, Piezoelectric Motors, an Overview, Actuators 5 (1) (2016) 6, https://doi.org/10.3390/act5010006, http://www.mdpi.com/2076-0825/5/1/6.
[7] Y. Liu, J. Deng, Q. Su, Review on Multi-Degree-of-Freedom Piezoelectric Motion Stage, IEEE Access 6 (2018) 59986–60004, https://doi.org/10.1109/ACCESS.2018.2875940.
[8] M.E. Kiziroglou, B. Temelkuran, E.M. Yeatman, G.Z. Yang, Micro Motion Amplification-A Review, IEEE Access 8 (2020) 64037–64055, https://doi.org/10.1109/ACCESS.2020.2984606.
[9] S. Wang, W. Rong, L. Wang, H. Xie, L. Sun, J.K. Mills, A survey of piezoelectric actuators with long working stroke in recent years: Classifications, principles, connections and distinctions (may 2019). doi:10.1016/j.ymssp.2019.01.033.
[10] L. Wang, W. Chen, J. Liu, J. Deng, Y. Liu, A review of recent studies on non-resonant piezoelectric actuators (nov 2019). doi:10.1016/j.ymssp.2019.106254. URL https://linkinghub.elsevier.com/retrieve/pii/S0888327019304698.
[11] H. Kulkarni, K. Zohaib, A. Khusru, K. Shravan Aiyappa, Application of piezoelectric technology in automotive systems, in: Mater. Today Proc., Vol. 5, Elsevier Ltd, 2018, pp. 21299–21304. doi:10.1016/j.matpr.2018.6.532.
[12] D. Kang, K. Kim, D. Kim, J. Shim, D.G. Gweon, J. Jeong, Optimal design of high precision XY-scanner with nanometer-level resolution and millimeter-level working range, Mechatronics 19 (4) (2009) 562–570, https://doi.org/10.1016/j.mechatronics.2009.01.002.
[13] H. Yu, Y. Liu, X. Tian, S. Zhang, J. Liu, A Precise Rotary Positioner Driven by Piezoelectric Bimorphs: Design, Analysis and Experimental Evaluation, Sensors Actuators A Phys. (2020) 112197, https://doi.org/10.1016/j.sna.2020.112197, https://linkinghub.elsevier.com/retrieve/pii/S0924424720303502.
[14] J. Peng, L. Ma, X. Li, H. Tang, Y. Li, S. Chen, A Novel Synchronous Micro Motor for Intravascular Ultrasound Imaging, IEEE Trans. Biomed. Eng. 66 (3) (2019) 802–809, https://doi.org/10.1109/TBME.2018.2856930.
[15] L. Wang, Y. Hou, K. Zhao, H. Shen, Z. Wang, C. Zhao, X. Lu, A novel piezoelectric inertial rotary motor for actuating micro underwater vehicles, Sensors Actuators, A Phys. 295 (2019) 428–438, https://doi.org/10.1016/j.sna.2019.06.014.
[16] W. Liang, J. Ma, C. Ng, Q. Ren, S. Huang, K.K. Tan, Optimal and intelligent motion control scheme for an Ultrasonic-Motor-Driven X-Y stage, Mechatronics 59 (2019) 127–139, https://doi.org/10.1016/j.mechatronics.2019.03.004.
[17] J. Stekke, C. Tendero, P. Tierce, C. Courtois, G. Rauwel, J. Lo, P. Guillot, F. Pigache, Low-voltage plasma jet with piezoelectric generator: Preliminary evaluation of decontamination capabilities, IEEE Trans. Plasma Sci. 48 (5) (2020) 1264–1270, https://doi.org/10.1109/TPS.2020.2985406.
[18] T. Sakayachi, Y. Nagira, M. Hikita, Study on achievement of simultaneous X, Y movements and theta rotation using straight-move ultrasonic vibrators, in: 2015 IEEE Int. Ultrason. Symp., IEEE, 2015, pp. 1–4. doi:10.1109/ULTSYM.2015.0539. URL http://ieeexplore.ieee.org/document/7329158/.
[19] C. Sun, G. Shang, Y. Tao, Z. Li, A review on application of piezoelectric energy harvesting technology, in: Adv. Mater. Res., Vol. 516–517, 2012, pp. 1481–1484. doi:10.4028/www.scientific.net/AMR.516-517.1481.
[20] G. Shang, Y. Tao, Z. Li, C. Sun, On piezoelectric harvesting technology, in: Adv. Mater. Res., Vol. 516–517, 2012, pp. 1496–1499. doi:10.4028/www.scientific.net/AMR.516-517.1496.
[21] H.F. Zhang, B. Wang, A.L. Zhao, Research on power supply for adaptive ultrasonic vibration cutting based on piezoelectric technology, Agro Food Ind. Hi. Tech. 28 (1) (2017) 2661–2665.
[22] M. Renaud, T. Sterken, A. Schmitz, P. Fiorini, C. Van Hoof, R. Puers, Piezoelectric harvesters and MEMS technology: Fabrication, modeling and measurements, in: TRANSDUCERS EUROSENSORS '07 - 4th Int. Conf. Solid-State Sensors, Actuators Microsystems, 2007, pp. 891–894. doi:10.1109/SENSOR.2007.4300274.
[23] D. Kuscer, T. Rojac, D. Belavič, M.S. Zarnik, A. Bradeško, T. Kos, B. Malič, M. Boerrigter, D.M. Martin, M. Faccini, Integrated piezoelectric vibration system for fouling mitigation in ceramic filtration membranes, J. Memb. Sci. 540 (2017) 277–284, https://doi.org/10.1016/j.memsci.2017.06.054.
[24] C.C. Chen, T.K. Chung, C.Y. Lin, A novel thermomagnetic-Actuated gripper with a piezoelectric-pyroelectric sensing readout of gripping states and forces, IEEE Trans. Magn. 53 (10). doi:10.1109/TMAG.2017.2731320.
[25] K.K. Sappati, S. Bhadra, Piezoelectric polymer and paper substrates: A review, Sensors (Switzerland) 18 (11). doi:10.3390/s18113605.
[26] B.P. Bruno, A.R. Fahmy, M. Stürmer, U. Wallrabe, M.C. Wapler, Properties of piezoceramic materials in high electric field actuator applications, Smart Mater. Struct. 28 (1). arXiv:1804.00192, doi:10.1088/1361-665X/aae8fb.
[27] H. Hoshyarmanesh, N. Ebrahimi, A. Jafari, P. Hoshyarmanesh, M. Kim, H.H. Park, PZT/PZT and PZT/BIT composite piezo-sensors in aerospace SHM applications: Photochemical metal organic + infiltration deposition and characterization, Sensors (Switzerland) 19 (1). doi:10.3390/s19010013.
[28] A. Mazzalai, D. Balma, N. Chidambaram, R. Matloub, P. Muralt, Characterization and Fatigue of the Converse Piezoelectric Effect in PZT Films for MEMS Applications, J. Microelectromechanical Syst. 24 (4) (2015) 831–838, https://doi.org/10.1109/JMEMS.2014.2353855.
[29] A. Daniels, M. Zhu, A. Tiwari, Evaluation of piezoelectric material properties for a higher power output from energy harvesters with insight into material selection using a coupled piezoelectric-circuit-finite element method, IEEE Trans. Ultrason. Ferroelectr. Freq. Control 60 (12) (2013) 2626–2633, https://doi.org/10.1109/TUFFC.2013.2861.
[30] U. Bachulska, J. Jankowska-Sumara, A. Majchrowski, M. Chrunik, D. Zasada, A. Soszyński, Thermal and dielectric properties of ferroelectric lead germanate single crystals doped with chromium ions (Pb5Ge3O11:Cr3+), Phase Transitions 91 (9–10) (2018) 923–931, https://doi.org/10.1080/01411594.2018.1507032.
[31] C. Liu, Q. Zhou, F.T. Djuth, K.K. Shung, High-frequency (>50 MHz) medical ultrasound linear arrays fabricated from micromachined bulk PZT materials, IEEE Trans. Ultrason. Ferroelectr. Freq. Control 59 (2) (2012) 315–318, https://doi.org/10.1109/TUFFC.2012.2193.
[32] S. Samanta, V. Sankaranarayanan, K. Sethupathi, Band gap, piezoelectricity and temperature dependence of differential permittivity and energy storage density of pzt with different zr/ti ratios, Vacuum 156 (2018) 456–462, https://doi.org/10.1016/j.vacuum.2018.08.015.
[33] M.J. Chrunik, S. Kłosowicz, P. Perkowski, M. Mrukiewicz, P. Morawiak, D. Zasada, The influence of microstructure and lattice strain on tetragonality factor and dielectric properties of ferroelectric ceramics BaTiO3, in: Acta Phys. Pol. A, Vol. 124, 2013, pp. 1034–1038. doi:10.12693/APhysPolA.124.1034.
[34] N.J. Donnelly, C.A. Randall, Impedance spectroscopy of PZT ceramics- measuring diffusion coefficients, mixed conduction, and Pb loss, IEEE Trans. Ultrason. Ferroelectr. Freq. Control 59 (9) (2012) 1883–1887, https://doi.org/10.1109/TUFFC.2012.2401.
[35] R.C. Da Silva Barros Allil, M.M. Werneck, Optical high-voltage sensor based on fiber bragg grating and PZT piezoelectric ceramics, IEEE Trans. Instrum. Meas. 60 (6) (2011) 2118–2125. doi:10.1109/TIM.2011.2115470.
[36] F. Khameneifar, S. Arzanpour, M. Moallem, A piezoelectric energy harvester for rotary motion applications: Design and experiments, IEEE/ASME Trans. Mechatronics 18 (5) (2013) 1527–1534, https://doi.org/10.1109/TMECH.2012.2205266.
[37] H. Huang, L. Wang, Y. Wu, Design and Experimental Research of a Rotary Micro-Actuator Based on a Shearing Piezoelectric Stack, Micromachines 10 (2) (2019) 96, https://doi.org/10.3390/mi10020096, http://www.mdpi.com/2072-666X/10/2/96.
[38] B. Nogarede, C. Henaux, J.-F. Rouchon, E. Duhayon, Electroactive materials: from piezomotors to electroactive morphing, in: IECON 2006–32nd Annual Conference on IEEE Industrial Electronics, 2006, pp. 4437–4441, https://doi.org/10.1109/IECON.2006.347918.
[39] V. Dabbagh, A.A. Sarhan, J. Akbari, N.A. Mardi, Design and experimental evaluation of a precise and compact tubular ultrasonic motor driven by a single-phase source, Precis. Eng. 48 (2017) 172–180, https://doi.org/10.1016/j.precisioneng.2016.11.018.
[40] R. Ryndzionek, Ł. Sienkiewicz, M. Michna, F. Kutt, Design and Experiments of a Piezoelectric Motor Using Three Rotating Mode Actuators, Sensors 19 (23) (2019) 5184, https://doi.org/10.3390/s19235184, https://www.mdpi.com/1424-8220/19/23/5184.
[41] M. Hunstig, Piezoelectric Inertia Motors A Critical Review of History, Concepts, Design, Applications, and Perspectives, Actuators 6 (1) (2017) 7, https://doi.org/10.3390/act6010007.
[42] T. Idogaki, H. Kanayama, N. Ohya, H. Suzuki, T. Hattori, Characteristics of piezoelectric locomotive mechanism for an in-pipe micro inspection machine, in: Proc. Int. Symp. Micro Mach. Hum. Sci., IEEE, 1995, pp. 193–198. doi:10.1109/mhs.1995.494237.
[43] Z. Zhakypov, E. Golubovic, T. Uzunovic, A. Sabanovic, High precision control of a walking piezoelectric motor in bending mode, in: 2013 9th Asian Control Conf. ASCC 2013, 2013, pp. 1–8. doi:10.1109/ASCC.2013.6606270.
[44] J.W. Judy, D.L. Polla, W.P. Robbins, A Linear Piezoelectric Stepper Motor with Submicrometer Step Size and Centimeter Travel Range, IEEE Trans. Ultrason. Ferroelectr. Freq. Control 37 (5) (1990) 428–437, https://doi.org/10.1109/58.105249.
[45] P. Vasiljev, D. Mazeika, Miniature flat type inertial piezoelectric motor, in: Proc. - IEEE Ultrason. Symp., Institute of Electrical and Electronics Engineers Inc., 2009, pp. 2607–2610. doi:10.1109/ULTSYM.2009.5441713.
[46] Y. Wang, S. Pan, W.Q. Huang, A linear stepping piezoelectric motor using inertial impact driving, in: Proc. 2011 Symp. Piezoelectricity, Acoust. Waves Device Appl. SPAWDA 2011, 2011, pp. 357–360. doi:10.1109/SPAWDA.2011.6167263.
[47] A.E. Glazounov, S. Wang, Q.M. Zhang, C. Kirn, Piezoelectric stepper motor with direct coupling mechanism to achieve high efficiency and precise control of motion, IEEE Trans. Ultrason. Ferroelectr. Freq. Control 47 (4) (2000) 1059–1067, https://doi.org/10.1109/58.852090.
[48] J. Twiefel, W. Wurpts, J. Wallaschek, Theoretical and experimental treatment of standing wave type motors contact behavior, in: Proc. - IEEE Ultrason. Symp., 2009, pp. 1–5, https://doi.org/10.1109/ULTSYM.2009.5442023.
[49] Y. Ting, Y.R. Tsai, B.K. Hou, S.C. Lin, C.C. Lu, Stator design of a new type of spherical piezoelectric motor, in: IEEE Trans. Ultrason. Ferroelectr. Freq. Control, Vol. 57, 2010, pp. 2334–2342. doi:10.1109/TUFFC.2010.1694.
[50] N. Fukaya, K. Sawada, H. Oku, H. Wada, S. Toyama, Development of an artificial arm by using a spherical ultrasonic motor, Seimitsu Kogaku Kaishi/Journal Japan Soc, Precis. Eng. 67 (4) (2001) 654–659, https://doi.org/10.2493/jjspe.67.654.
[51] Y. Ma, M. Choi, K. Uchino, Single-phase driven ultrasonic motor using two orthogonal bending modes of sandwiching piezo-ceramic plates, Rev. Sci. Instrum. 87 (11) (2016) 115004, https://doi.org/10.1063/1.4967857.
[52] S. Zhang, Y. Liu, J. Deng, X. Tian, X. Gao, Development of a two-DOF inertial rotary motor using a piezoelectric actuator constructed on four bimorphs, Mech. Syst. Signal Process. 149 (2021) 107213, https://doi.org/10.1016/j.ymssp.2020.107213, https://linkinghub.elsevier.com/retrieve/pii/S0888327020305999.
[53] Y. Liu, L. Wang, Z. Gu, Q. Quan, J. Deng, Development of a Two-Dimensional Linear Piezoelectric Stepping Platform Using Longitudinal-Bending Hybrid

Actuators, IEEE Trans. Ind. Electron. 66 (4) (2019) 3030–3040, https://doi.org/10.1109/TIE.2018.2842730.
[54] L. Petit, P. Gonnard, A multilayer TWILA ultrasonic motor, Sensors Actuators, A Phys. 149 (1) (2009) 113–119, https://doi.org/10.1016/j.sna.2008.09.020.
[55] D.A. Stepanenko, V.T. Minchenya, Development and study of novel non-contact ultrasonic motor based on principle of structural asymmetry, Ultrasonics 52 (7) (2012) 866–872, https://doi.org/10.1016/j.ultras.2012.02.004.
[56] W. Qiu, Y. Hong, Y. Mizuno, W. Wen, K. Nakamura, Non-contact piezoelectric rotary motor modulated by giant electrorheological fluid, Sensors Actuators, A Phys. 217 (2014) 124–128, https://doi.org/10.1016/j.sna.2014.05.019.
[57] T. Peng, H. Shi, X. Liang, F. Luo, X. Wu, Experimental investigation on sandwich structure ring-type ultrasonic motor, Ultrasonics 56 (2015) 303–307, https://doi.org/10.1016/j.ultras.2014.08.014.
[58] M. Shi, X. Liu, K. Feng, K. Zhang, Experimental and numerical investigation of a self-adapting non-contact ultrasonic motor, Tribol. Int. 153 (2021) 106624, https://doi.org/10.1016/j.triboint.2020.106624.
[59] W. Seemann, A linear ultrasonic traveling wave motor of the ring type, Smart Mater. Struct. 5 (3) (1996) 361–368, https://doi.org/10.1088/0964-1726/5/3/015, https://iopscience.iop.org/article/10.1088/0964-1726/5/3/015 https://iopscience.iop.org/article/10.1088/0964-1726/5/3/015/meta.
[60] G.L. Smith, R.Q. Rudy, R.G. Polcawich, D.L. Devoe, Integrated thin-film piezoelectric traveling wave ultrasonic motors, in: Sensors Actuators, A Phys., Vol. 188, Elsevier, 2012, pp. 305–311. doi:10.1016/j.sna.2011.12.029.
[61] R.Q. Rudy, G.L. Smith, D.L. DeVoe, R.G. Polcawich, Millimeter-scale traveling wave rotary ultrasonic motors, J. Microelectromechanical Syst. 24 (1) (2015) 108–114, https://doi.org/10.1109/JMEMS.2014.2317778.
[62] J. Zhang, L. Yang, H. Chen, C. Ma, X. Shen, L. Chen, Design of Travelling-Wave Rotating Ultrasonic Motor under High Overload Environments: Impact Dynamics Simulation and Experimental Validation, Appl. Sci. 9 (24) (2019) 5309, https://doi.org/10.3390/app9245309, https://www.mdpi.com/2076-3417/9/24/5309.
[63] SHINSEI Corporation—Top (2020). http://www.shinsei-motor.com/English/.
[64] W. Wang, Y. Shi, X. Yuan, A. Goldenberg, P. Shokrollahi, Compatibility of US motors for development of MRI-guided surgical robot, in: Proc. 2013 6th Int. Conf. Biomed. Eng. Informatics, BMEI 2013, IEEE Computer Society, 2013, pp. 388–392. doi:10.1109/BMEI.2013.6746969.
[65] E. Mujjalinvimut, M. Konghirun, P. Laoratanakul, A design study of ultrasonic motor drive, in: 2009 6th Int. Conf. Electr. Eng. Comput. Telecommun. Inf. Technol. ECTI-CON 2009, Vol. 1, 2009, pp. 274–277. doi:10.1109/ECTICON.2009.5137007.
[66] A. Kumada, A piezoelectric ultrasonic motor, Jpn. J. Appl. Phys. 24 (S2) (1985) 739–741, https://doi.org/10.7567/JJAPS.24S2.739, https://iopscience.iop.org/article/10.7567/JJAPS.24S2.739 https://iopscience.iop.org/article/10.7567/JJAPS.24S2.739/meta.
[67] K. Uchino, Piezoelectric motors for camera modules, in: Proc. 11th Int. Conf. New Actuators, 2008, pp. 157–160.
[68] T. Mashimo, K. Terashima, Experimental verification of elliptical motion model in traveling wave ultrasonic motors, IEEE/ASME Trans. Mechatronics 20 (6) (2015) 2699–2707, https://doi.org/10.1109/TMECH.2015.2392126.
[69] F. Giraud, B. Semail, J.T. Audren, Analysis and phase control of a piezoelectric traveling-wave ultrasonic motor for haptic stick application, IEEE Trans. Ind. Appl. 40 (6) (2004) 1541–1549, https://doi.org/10.1109/TIA.2004.836317.
[70] J. Li, S. Liu, N. Zhou, A. Yu, Y. Cui, P. Chen, A traveling wave ultrasonic motor with a metal/polymer-matrix material compound stator, Smart Mater. Struct. 27 (1) (2018) 015027, https://doi.org/10.1088/1361-665X/aa9cc4.
[71] I.A. Renteria-Marquez, A. Renteria-Marquez, B.T. Tseng, A novel contact model of piezoelectric traveling wave rotary ultrasonic motors with the finite volume method, Ultrasonics 90 (2018) 5–17, https://doi.org/10.1016/j.ultras.2018.06.004.
[72] W. Zeng, S. Pan, L. Chen, Z. Xu, Z. Xiao, J. Zhang, Research on ultra-low speed driving method of traveling wave ultrasonic motor for CMG, Ultrasonics 103 (2020) 106088, https://doi.org/10.1016/j.ultras.2020.106088.
[73] Y. Zhou, J. Chang, X. Liao, Z. Feng, Ring-shaped traveling wave ultrasonic motor for high-output power density with suspension stator, Ultrasonics 102 (2020) 106040, https://doi.org/10.1016/j.ultras.2019.106040.
[74] S. Li, W. Ou, M. Yang, C. Guo, C. Lu, J. Hu, Temperature evaluation of traveling-wave ultrasonic motor considering interaction between temperature rise and motor parameters, Ultrasonics 57 (C) (2015) 159–166, https://doi.org/10.1016/j.ultras.2014.11.007.
[75] H. Chen, C. Chen, J. Wang, M. Shi, Performance analysis and experimental study of traveling wave type rotary ultrasonic motor in high-rotation environment, Rev. Sci. Instrum. 89 (11) (2018) 115004, https://doi.org/10.1063/1.5055579, http://aip.scitation.org/doi/10.1063/1.5055579.
[76] T. Sattel, P. Hagedorn, J. Schmidt, The contact problem in ultrasonic traveling-wave motors, J. Appl. Mech. Trans. ASME 77 (3) (2010) 1–11, https://doi.org/10.1115/1.4000380.
[77] X. Ma, J. Liu, J. Deng, Q. Liu, Y. Liu, A Rotary Traveling Wave Ultrasonic Motor with Four Groups of Nested PZT Ceramics: Design and Performance Evaluation, IEEE Trans. Ultrason. Ferroelectr. Freq. Control (2020) 1, https://doi.org/10.1109/tuffc.2020.2972307.
[78] W. Chen, Y. Liu, X. Yang, J. Liu, Ring-type traveling wave ultrasonic motor using a radial bending mode, IEEE Trans. Ultrason. Ferroelectr. Freq. Control 61 (1) (2014) 197–202, https://doi.org/10.1109/TUFFC.2014.6689788.
[79] Y. Zhao, S. Yuan, X. Chu, S. Gao, Z. Zhong, C. Zhu, Ultrasonic micro-motor with multilayer piezoelectric ceramic and chamfered driving tips, Rev. Sci. Instrum. 87 (9) (2016) 095108, https://doi.org/10.1063/1.4963662.
[80] L. Wang, Y. Wang, X. Lu, C. Zhao, Note: A disk-shaft shaped high-speed rotary ultrasonic motor, Rev. Sci. Instrum. 89 (12) (2018) 126106, https://doi.org/10.1063/1.5065427, http://aip.scitation.org/doi/10.1063/1.5065427.
[81] X. Dong, M. Hu, L. Jin, Z. Xu, C. Jiang, A standing wave ultrasonic stepping motor using open-loop control system, Ultrasonics 82 (2018) 327–330, https://doi.org/10.1016/j.ultras.2017.09.014.
[82] C. Jiang, X. Dong, L. Jin, D. Lu, Contact Modeling and Performance Evaluation of a Radial Standing Wave Ultrasonic Motor, Math. Probl. Eng. (2019), https://doi.org/10.1155/2019/1093108.
[83] D. Bai, Q. Quan, D. Tang, Z. Deng, Design and Experiments of a Novel Rotary Piezoelectric Actuator Using Longitudinal-Torsional Convertors, IEEE Access 7 (2019) 22186–22195, https://doi.org/10.1109/ACCESS.2019.2898262.
[84] M. Kurosawa, K. Nakamura, T. Okamoto, S. Ueha, An Ultrasonic Motor Using Bending Vibrations of a Short Cylinder, IEEE Trans. Ultrason. Ferroelectr. Freq. Control 36 (5) (1989) 517–521, https://doi.org/10.1109/58.31795.
[85] L. Han, L. Yu, C. Pan, H. Zhao, Y. Jiang, A Novel Impact Rotary-Linear Motor Based on Decomposed Screw-Type Motion of Piezoelectric Actuator, Appl. Sci. 8 (12) (2018) 2492, https://doi.org/10.3390/app8122492, http://www.mdpi.com/2076-3417/8/12/2492.
[86] Y. Liu, W. Chen, J. Liu, X. Yang, A high-power linear ultrasonic motor using bending vibration transducer, IEEE Trans. Ind. Electron. 60 (11) (2013) 5160–5166, https://doi.org/10.1109/TIE.2012.2233691.
[87] L. Petit, P. Gonnard, Industrial design of a centimetric TWILA ultrasonic motor, Sensors Actuators, A Phys. 120 (1) (2005) 211–224, https://doi.org/10.1016/j.sna.2004.11.018.
[88] T. Mashimo, Micro Ultrasonic Motor Using a Cube with a Side Length of 0.5 mm, IEEE/ASME Trans. Mechatronics 21 (2) (2016) 1189–1192. doi:10.1109/TMECH.2015.2511782.
[89] T. Mashimo, S. Izuhara, S. Arai, Z. Zhang, H. Oku, High-Speed Visual Feedback Control of Miniature Rotating Mirror System Using a Micro Ultrasonic Motor, IEEE Access 8 (2020) 38546–38553, https://doi.org/10.1109/ACCESS.2019.2957298.
[90] J. Wu, Y. Mizuno, K. Nakamura, Piezoelectric Motor Utilizing an Alumina/PZT Transducer, IEEE Trans. Ind. Electron. 67 (8) (2020) 6762–6772, https://doi.org/10.1109/TIE.2019.2937047.
[91] C. Li, C. yue Lu, Y. xin Ma, S. yang Li, W. qing Huang, Design of an ultrasonic motor with multi-vibrators, J. Zhejiang Univ. Sci. A 17 (9) (2016) 724–732. doi: 10.1631/jzus.A1500316. doi: 10.1631/jzus.A1500316.
[92] X. Yang, Y. Liu, W. Chen, J. Liu, A cylindrical traveling wave ultrasonic motor using bonded-type composite beam, Ultrasonics 65 (2016) 277–281, https://doi.org/10.1016/j.ultras.2015.09.014.
[93] Y. Liu, W. Chen, J. Liu, S. Shi, A cylindrical traveling wave ultrasonic motor using longitudinal and bending composite transducer, Sensors Actuators, A Phys. 161 (1–2) (2010) 158–163, https://doi.org/10.1016/j.sna.2010.06.001.
[94] Y. Liu, W. Chen, P. Feng, J. Liu, A rotary piezoelectric motor using bending vibrators, Sensors Actuators, A Phys. 196 (2013) 48–54, https://doi.org/10.1016/j.sna.2013.03.035.
[95] L. Yang, W. Ren, C. Ma, L. Chen, Mechanical simulation and contact analysis of the hybrid longitudinal-torsional ultrasonic motor, Ultrasonics 100 (2020) 105982, https://doi.org/10.1016/j.ultras.2019.105982.
[96] R. Ryndzionek, M. Michna, M. Ronkowski, J.F. Rouchon, Chosen Analysis Results of the Prototype Multicell Piezoelectric Motor, IEEE/ASME Trans. Mechatronics 23 (5) (2018) 2178–2185, https://doi.org/10.1109/TMECH.2018.2865619.
[97] P. Hareesh, D.L. DeVoe, Miniature Bulk PZT Traveling Wave Ultrasonic Motors for Low-Speed High-Torque Rotary Actuation, J. Microelectromechanical Syst. 27 (3) (2018) 547–554, https://doi.org/10.1109/JMEMS.2018.2823980.
[98] V. Dabbagh, A.A. Sarhan, J. Akbari, N.A. Mardi, Design and manufacturing of ultrasonic motor with in-plane and out-of-plane bending vibration modes of rectangular plate with large contact area, Meas. J. Int. Meas. Confed. 109 (2017) 425–431, https://doi.org/10.1016/j.measurement.2017.06.007.
[99] D. Xu, Y. Liu, J. Liu, W. Chen, A Bonded Type Ultrasonic Motor Using the Bending of a Crossbeam, IEEE Access 4 (2016) 1109–1116, https://doi.org/10.1109/ACCESS.2016.2542861.
[100] Y. Liu, X. Yang, W. Chen, D. Xu, A Bonded-Type Piezoelectric Actuator Using the First and Second Bending Vibration Modes, IEEE Trans. Ind. Electron. 63 (3) (2016) 1676–1683, https://doi.org/10.1109/TIE.2015.2492942.
[101] T. Peng, X. Wu, X. Liang, H. Shi, F. Luo, Investigation of a rotary ultrasonic motor using a longitudinal vibrator and spiral fin rotor, Ultrasonics 61 (2015) 157–161, https://doi.org/10.1016/j.ultras.2015.04.013.
[102] S. Arnold, Technical Progress with Ultrasonic Piezomotors, PI News (2009) 1–8, http://www.pi-newsletter.net/pdf/PI-News-40.pdf.
[103] G.B. Bremen, M.F. Six, R. Le Letty, P. Coste, F. Claeyssen, Rotating step by step piezomotor for nanopositioning & space applications, in: ACTUATOR 2006, 10th International Conference on New Actuators, 2006, pp. 14–16.
[104] Z. Liu, Z. Yao, X. Li, Q. Fu, Design and experiments of a linear piezoelectric motor driven by a single mode, Rev. Sci. Instrum. 87 (11) (2016) 115001, https://doi.org/10.1063/1.4966251, http://aip.scitation.org/doi/10.1063/1.4966251.
[105] B. Zhang, Z. Yao, Z. Liu, X. Li, A novel L-shaped linear ultrasonic motor operating in a single resonance mode, Rev. Sci. Instrum. 89 (1) (2018) 015006, https://doi.org/10.1063/1.5011427, http://aip.scitation.org/doi/10.1063/1.5011427.
[106] S. He, W. Chen, X. Tao, Z. Chen, Standing wave Bi-directional linearly moving ultrasonic motor, IEEE Trans. Ultrason. Ferroelectr. Freq. Control 45 (5) (1998) 1133–1139, https://doi.org/10.1109/58.726435.
[107] L. Han, L. Yu, C. Pan, Y. Jiang, A compact linear-rotary impact motor based on a single piezoelectric tube stator with two independent electrodes, Rev. Sci.

Instrum. 90 (11) (2019) 115004, https://doi.org/10.1063/1.5109835, http://aip.scitation.org/doi/10.1063/1.5109835.
[108] M. Morawiec, K. Blecharz, A. Lewicki, Sensorless rotor position estimation of doubly fed induction generator based on backstepping technique, IEEE Trans. Ind. Electron. 67 (7) (2020) 5889–5899, https://doi.org/10.1109/TIE.2019.2955403.
[109] S. Zhou, Z. Yao, Design and optimization of a modal-independent linear ultrasonic motor, IEEE Trans. Ultrason. Ferroelectr. Freq. Control 61 (3) (2014) 535–546, https://doi.org/10.1109/TUFFC.2014.2937.
[110] M. Guo, S. Pan, J. Hu, C. Zhao, S. Dong, A small linear ultrasonic motor utilizing longitudinal and bending modes of a piezoelectric tube, IEEE Trans. Ultrason. Ferroelectr. Freq. Control 61 (4) (2014) 705–709, https://doi.org/10.1109/TUFFC.2014.2958.
[111] L. Jarzebowicz, Errors of a Linear Current Approximation in High-Speed PMSM Drives, IEEE Trans. Power Electron. 32 (11) (2017) 8254–8257, https://doi.org/10.1109/TPEL.2017.2694450.
[112] D. Wachowiak, Genetic Algorithm Approach for Gains Selection of Induction Machine Extended Speed Observer, Energies 13 (18) (2020) 4632, https://doi.org/10.3390/en13184632, https://www.mdpi.com/1996-1073/13/18/4632.
[113] P. Dworakowski, A. Wilk, M. Michna, A. Fouineau, M. Guillet, Lagrangian model of an isolated dc-dc converter with a 3-phase medium frequency transformer accounting magnetic cross saturation, IEEE Trans. Power Deliv. (2020) 1, https://doi.org/10.1109/tpwrd.2020.2995879.
[114] X. Tian, B. Zhang, Y. Liu, S. Chen, H. Yu, A novel U-shaped stepping linear piezoelectric actuator with two driving feet and low motion coupling: Design, modeling and experiments, Mech. Syst. Signal Process. 124 (2019) 679–695, https://doi.org/10.1016/j.ymssp.2019.02.019.
[115] S. Xie, C. Ni, H. Duan, Y. Liu, N. Qi, Hybrid model based on the maxwell-slip model and a support vector machine for hysteresis in piezoelectric actuators, in: 2020 IEEE/ASME International Conference on Advanced Intelligent Mechatronics (AIM), 2020, pp. 36–41, https://doi.org/10.1109/AIM43001.2020.9158982.
[116] X. Li, C. Kan, Y. Cheng, Z. Chen, T. Ren, Performance evaluation of a bimodal standing-wave ultrasonic motor considering nonlinear electroelasticity: Modeling and experimental validation, Mech. Syst. Signal Process. 141 (2020) 106475, https://doi.org/10.1016/j.ymssp.2019.106475.
[117] X. Li, Y. Huang, L. Zhou, Integrated performance improvement for a bimodal linear ultrasonic motor using a dual-frequency asymmetric excitation method, Ultrasonics 108 (2020) 106224, https://doi.org/10.1016/j.ultras.2020.106224.
[118] X. Li, Z. Yao, Y. He, S. Dai, Modeling and experimental investigation of thermal-mechanical-electric coupling dynamics in a standing wave ultrasonic motor, Smart Mater. Struct. 26 (9) (2017) 095044, https://doi.org/10.1088/1361-665X/aa7bc9.
[119] S. He, S. Shi, Y. Zhang, W. Chen, Design and experimental research on a deep-sea resonant linear ultrasonic motor, IEEE Access 6 (2018) 57249–57256, https://doi.org/10.1109/ACCESS.2018.2873745.
[120] S. Shao, S. Shi, W. Chen, J. Liu, Y. Liu, Research on a Linear Piezoelectric Actuator Using T-Shape Transducer to Realize High Mechanical Output, Appl. Sci. 6 (4) (2016) 103, https://doi.org/10.3390/app6040103, http://www.mdpi.com/2076-3417/6/4/103.
[121] Y. Liu, W. Chen, J. Liu, S. Shi, A high-power linear ultrasonic motor using longitudinal vibration transducers with single foot, IEEE Trans. Ultrason. Ferroelectr. Freq. Control 57 (8) (2010) 1860–1867, https://doi.org/10.1109/TUFFC.2010.1625.
[122] J. Niu, J. Wu, M. Cao, L. Wu, A Traveling-Wave Linear Ultrasonic Motor Driven by Two Torsional Vibrations: Design, Fabrication, and Performance Evaluation, IEEE Access 8 (2020) 122554–122564, https://doi.org/10.1109/ACCESS.2020.3006888, https://ieeexplore.ieee.org/document/9133076/.
[123] X. Li, P. Ci, G. Liu, S. Dong, A two-layer linear piezoelectric micromotor, IEEE Trans. Ultrason. Ferroelectr. Freq. Control 62 (3) (2015) 405–411, https://doi.org/10.1109/TUFFC.2014.006796.
[124] J. Liu, Y. Liu, L. Zhao, D. Xu, W. Chen, J. Deng, Design and Experiments of a Single-Foot Linear Piezoelectric Actuator Operated in a Stepping Mode, IEEE Trans. Ind. Electron. 65 (10) (2018) 8063–8071, https://doi.org/10.1109/TIE.2018.2798627.
[125] R. Niu, H. Zhu, C. Zhao, A four-legged linear ultrasonic motor: Design and experiments, Rev. Sci. Instrum. 91 (7) (2020) 076107, https://doi.org/10.1063/1.5114787, http://aip.scitation.org/doi/10.1063/1.5114787.
[126] Y. Tanoue, T. Morita, Opposing preloads type ultrasonic linear motor with quadruped stator, Sensors Actuators, A Phys. 301 (2020) 111764, https://doi.org/10.1016/j.sna.2019.111764.
[127] Z. Yin, C. Dai, Z. Cao, W. Li, Z. Chen, C. Li, Modal analysis and moving performance of a single-mode linear ultrasonic motor, Ultrasonics 108 (2020) 106216, https://doi.org/10.1016/j.ultras.2020.106216.
[128] L. Wang, J. Liu, Y. Liu, X. Tian, J. Yan, A novel single-mode linear piezoelectric ultrasonic motor based on asymmetric structure, Ultrasonics 89 (2018) 137–142, https://doi.org/10.1016/j.ultras.2018.05.010.
[129] J. Yan, Y. Liu, J. Liu, D. Xu, W. Chen, The design and experiment of a novel ultrasonic motor based on the combination of bending modes, Ultrasonics 71 (2016) 205–210, https://doi.org/10.1016/j.ultras.2016.07.002.
[130] G. Rogers, Three degree-of-freedom piezoelectric ultrasonic micro-motor with a major diameter of 350 μm, J. Micromechanics Microengineering 20 (12) (2010) 5, https://doi.org/10.1088/0960-1317/20/12/125002, https://iopscience.iop.org/article/10.1088/0960-1317/20/12/125002 https://iopscience.iop.org/article/10.1088/0960-1317/20/12/125002/meta.
[131] Y. Liu, W. Chen, J. Liu, S. Shi, A cylindrical standing wave ultrasonic motor using bending vibration transducer, Ultrasonics 51 (5) (2011) 527–531, https://doi.org/10.1016/j.ultras.2010.12.007.
[132] B. Keller, W. Schinkoethe, Multi-degree-of-freedom ultrasonic motors using rotation-symmetric piezoelectric vault geometries - VDE Conference Publication, in: Innov. Small Drives Micro-Motor Syst., Nuremberg, Germany, 2013, pp. 1–6. https://ieeexplore.ieee.org/document/6624087.
[133] X. Gao, S. Zhang, J. Deng, Y. Liu, Development of a Small Two-Dimensional Robotic Spherical Joint Using a Bonded-Type Piezoelectric Actuator, IEEE Trans. Ind. Electron. (2019) 1, https://doi.org/10.1109/tie.2019.2959475.
[134] V. Jurenas, G. Kazokaitis, D. Mažeika, Design of Unimorph Type 3DOF Ultrasonic Motor, Appl. Sci. 10 (16) (2020) 5605, https://doi.org/10.3390/app10165605, https://www.mdpi.com/2076-3417/10/16/5605.
[135] B. Lv, G. Wang, B. Li, H. Zhou, Y. Hu, Research on a 3-DOF Motion Device Based on the Flexible Mechanism Driven by the Piezoelectric Actuators, Micromachines 9 (11) (2018) 578, https://doi.org/10.3390/mi9110578, http://www.mdpi.com/2072-666X/9/11/578.
[136] M. Hu, H. Du, S.F. Ling, J.K. Teo, A piezoelectric spherical motor with two degree-of-freedom, Sensors Actuators, A Phys. 94 (1–2) (2001) 113–116, https://doi.org/10.1016/S0924-4247(01)00671-9.
[137] W.M. Chen, T.S. Liu, Modeling and experimental validation of new two degree-of-freedom piezoelectric actuators, Mechatronics 23 (8) (2013) 1163–1170, https://doi.org/10.1016/j.mechatronics.2013.10.002.
[138] T. Mashimo, S. Toyama, H. Ishida, Design and implementation of spherical ultrasonic motor, IEEE Trans. Ultrason. Ferroelectr. Freq. Control 56 (11) (2009) 2514–2521, https://doi.org/10.1109/TUFFC.2009.1338.
[139] L. Yan, Y. Hu, H. Lan, N. Yao, Z. Jiao, I.M. Chen, A novel two degree-of-freedom ultrasonic planar motor driven by single stator, in: IEEE Int. Conf. Ind. Informatics, 2012, pp. 550–553, https://doi.org/10.1109/INDIN.2012.6301369.
[140] V. Jurenas, G. Kazokaitis, D. Mažeika, 3DOF Ultrasonic Motor with Two Piezoelectric Rings, Sensors 20 (3) (2020) 834, https://doi.org/10.3390/s20030834, https://www.mdpi.com/1424-8220/20/3/834.
[141] S. Toyama, S. Hatae, M. Nonaka, Development of multi-degree of freedom spherical ultrasonic motor, in: Fifth International Conference on Advanced Robotics 'Robots in Unstructured Environments, Institute of Electrical and Electronics Engineers (IEEE), 1991, pp. 55–60 vol 1. doi:10.1109/icar.1991.240476.
[142] T. Shigeki, S. Shigeru, Z. Guoqiang, M. Yasutaro, N. Kazuto, Multi degree of freedom spherical ultrasonic motor, in: Proc. - IEEE Int. Conf. Robot. Autom., Vol. 3, IEEE, 1995, pp. 2935–2940. doi:10.1109/robot.1995.525700.
[143] Z. Huang, S. Shi, W. Chen, L. Wang, L. Wu, Y. Liu, Development of a novel spherical stator multi-DOF ultrasonic motor using in-plane non-axisymmetric mode, Mech. Syst. Signal Process. 140 (2020) 106658, https://doi.org/10.1016/j.ymssp.2020.106658.
[144] Z. Li, Z. Wang, P. Guo, L. Zhao, Q. Wang, A ball-type multi-DOF ultrasonic motor with three embedded traveling wave stators, Sensors Actuators, A Phys. 313 (2020) 112161, https://doi.org/10.1016/j.sna.2020.112161.
[145] Z. Li, Z. Wang, L. Zhao, P. Guo, Characteristic Analysis and Experimental Study of Spherical Ultrasonic Motor with Multi-degree-of-freedom, J. Appl. Sci. Eng. 23 (4) (2020) 619–626, https://doi.org/10.6180/jase.202012_23.
[146] S. Shi, H. Xiong, Y. Liu, W. Chen, J. Liu, A ring-type multi-DOF ultrasonic motor with four feet driving consistently, Ultrasonics 76 (2017) 234–244, https://doi.org/10.1016/j.ultras.2017.01.005.
[147] L. Yan, D. Liu, H. Lan, Z. Jiao, Compact traveling wave micromotor based on shear electromechanical coupling, IEEE/ASME Trans. Mechatronics 21 (3) (2016) 1572–1580, https://doi.org/10.1109/TMECH.2016.2524585.
[148] X. Yang, Y. Liu, W. Chen, J. Liu, Sandwich-Type Multi-Degree-of-Freedom Ultrasonic Motor with Hybrid Excitation, IEEE Access 4 (2016) 905–913, https://doi.org/10.1109/ACCESS.2016.2536611.
[149] L. Yan, H. Lan, Z. Jiao, C.-Y. Chen, I.-M. Chen, Compact piezoelectric micromotor with a single bulk lead zirconate titanate stator, Applied Physics Letters 102 (13) (2013) 134106. arXiv:https://doi.org/10.1063/1.4799353, doi:10.1063/1.4799353. doi: 10.1063/1.4799353.
[150] H. Li, L. Wang, T. Cheng, M. He, H. Zhao, H. Gao, A High-Thrust Screw-Type Piezoelectric Ultrasonic Motor with Three-Wavelength Exciting Mode, Appl. Sci. 6 (12) (2016) 442, https://doi.org/10.3390/app6120442, http://www.mdpi.com/2076-3417/6/12/442.
[151] Y. Wang, Q. Quan, H. Yu, D. Bai, H. Li, Z. Deng, Rotary-percussive ultrasonic drill: An effective subsurface penetrating tool for minor planet exploration, IEEE Access 6 (2018) 37796–37806, https://doi.org/10.1109/ACCESS.2018.2853166.
[152] S. Shi, Z. Huang, J. Yang, Y. Liu, W. Chen, K. Uchino, Development of a compact ring type MDOF piezoelectric ultrasonic motor for humanoid eyeball orientation system, Sensors Actuators, A Phys. 272 (2018) 1–10, https://doi.org/10.1016/j.sna.2017.12.031.
[153] J. Yan, Y. Liu, S. Shi, W. Chen, A three-DOF ultrasonic motor using four piezoelectric ceramic plates in bonded-type structure, J. Vibroengineering 20 (1) (2018) 358–367, https://doi.org/10.21595/jve.2017.18523, https://doi.org/10.21595/jve.2017.18523.
[154] L. Wang, Q. Quan, K. Xue, H. Li, Development of a three-dof piezoelectric actuator using a thin cross-beam vibrator, Int. J. Mech. Sci. 149 (2018) 54–61, https://doi.org/10.1016/j.ijmecsci.2018.09.039.
[155] J. Wang, X. xing Hu, B. Wang, J. feng Guo, A novel two-degree-of-freedom spherical ultrasonic motor using three travelling-wave type annular stators, J. Cent. South Univ. 22 (4) (2015) 1298–1306. doi:10.1007/s11771-015-2646-z. https://link.springer.com/article/10.1007/s11771-015-2646-z.
[156] D. Xu, Y. Liu, J. Liu, X. Yang, W. Chen, Developments of a piezoelectric actuator with nano-positioning ability operated in bending modes, Ceram. Int. 43 (2017) S21–S26, https://doi.org/10.1016/j.ceramint.2017.05.199.

[157] T. Nishimura, H. Hosaka, T. Morita, Resonant-type Smooth Impact Drive Mechanism (SIDM) actuator using a bolt-clamped Langevin transducer, Ultrasonics 52 (1) (2012) 75–80, https://doi.org/10.1016/j.ultras.2011.06.013.
[158] Q.S. Pan, L.G. He, C.L. Pan, G.J. Xiao, Z.H. Feng, Resonant-type inertia linear motor based on the harmonic vibration synthesis of piezoelectric bending actuator, Sensors Actuators, A Phys. 209 (2014) 169–174, https://doi.org/10.1016/j.sna.2014.01.027.
[159] H. Yokozawa, Y. Doshida, S. Kishimoto, T. Morita, Resonant-type smooth impact drive mechanism actuator using lead-free piezoelectric material, Sensors Actuators, A Phys. 274 (2018) 179–183, https://doi.org/10.1016/j.sna.2018.02.012.
[160] J. Deng, Y. Liu, J. Liu, D. Xu, Y. Wang, Development of a planar piezoelectric actuator using bending-bending hybrid transducers, IEEE Trans. Ind. Electron. 66 (8) (2019) 6141–6149, https://doi.org/10.1109/TIE.2018.2873123.
[161] J. Li, H. Liu, H. Zhao, A Compact 2-DOF Piezoelectric-Driven Platform Based on "Z-Shaped" Flexure Hinges, Micromachines 8 (8) (2017) 245, https://doi.org/10.3390/mi8080245, http://www.mdpi.com/2072-666X/8/8/245.
[162] S.C. Shen, Y.C. Chen, Design and evaluation of a multi-degree-of-freedom piezoelectric microactuator and its applications, Int. J. Autom. Smart Technol. 3 (4) (2013) 251–257, https://doi.org/10.5875/ausmt.v3i4.208.
[163] J. Deng, Y. Liu, K. Li, Q. Su, H. Yu, A novel planar piezoelectric actuator with nano-positioning ability operating in bending-bending hybrid modes, Ceram. Int. 44 (2018) S164–S167, https://doi.org/10.1016/j.ceramint.2018.08.123.
[164] H. Hariri, Y. Bernard, A. Razek, 2-D traveling wave driven piezoelectric plate robot for planar motion, IEEE/ASME Trans. Mechatronics 23 (1) (2018) 242–251, https://doi.org/10.1109/TMECH.2018.2791508.
[165] Y. Liu, J. Yan, L. Wang, W. Chen, A Two-DOF Ultrasonic Motor Using a Longitudinal-Bending Hybrid Sandwich Transducer, IEEE Trans. Ind. Electron. 66 (4) (2019) 3041–3050, https://doi.org/10.1109/TIE.2018.2847655.
[166] X. Zhou, W. Chen, J. Liu, Novel 2-DOF Planar Ultrasonic Motor with Characteristic of Variable Mode Excitation, IEEE Trans. Ind. Electron. 63 (11) (2016) 6941–6948, https://doi.org/10.1109/TIE.2016.2586018.
[167] Y. Sato, A. Kanada, T. Mashimo, Self-Sensing and Feedback Control for a Twin Coil Spring-Based Flexible Ultrasonic Motor, IEEE Robot. Autom. Lett. 5 (4) (2020) 5425–5431, https://doi.org/10.1109/LRA.2020.3008118.
[168] Z. Chen, X. Li, G. Liu, S. Dong, A two degrees-of-freedom piezoelectric single-crystal micromotor, J. Appl. Phys. 116 (22) (2014) 224101, https://doi.org/10.1063/1.4903834, http://aip.scitation.org/doi/10.1063/1.4903834.
[169] T. Hirano, M. Aoyagi, H. Kajiwara, H. Tamura, T. Takano, Development of rotary-type noncontact-synchronous ultrasonic motor Recent citations Experimental and numerical investigation of a self-adapting non-contact ultrasonic motor Minghui Shi et al-High-power properties of (Sr,Ca) 2 NaNb 5 O 15 piezoelectric cer, Jpn. J. Appl. Phys.doi:10.7567/1347-4065/ab1bd5. URL https://doi.org/10.7567/1347-4065/ab1bd5.
[170] M.A. Tavallaei, S.F. Atashzar, M. Drangova, Robust Motion Control of Ultrasonic Motors under Temperature Disturbance, IEEE Trans. Ind. Electron. 63 (4) (2016) 2360–2368, https://doi.org/10.1109/TIE.2015.2499723.
[171] W. Shi, H. Zhao, J. Ma, Y. Yao, An Optimum-Frequency Tracking Scheme for Ultrasonic Motor, IEEE Trans. Ind. Electron. 64 (6) (2017) 4413–4422, https://doi.org/10.1109/TIE.2017.2674612.